NASA TECHNICAL NOTE

NASA TN D-3171

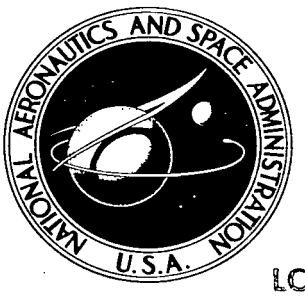

NASA TN D-3171

SUPERSONIC FLUTTER OF SIMPLY SUPPORTED ISOTROPIC SANDWICH PANELS

by Larry L. Erickson and Melvin S. Anderson

Langley Research Center
Langley Station, Hampton, Va.

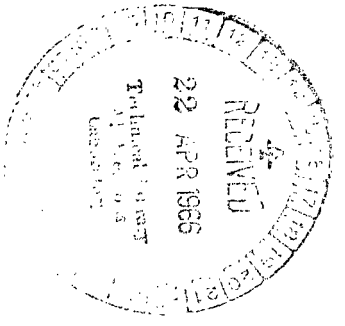

NATIONAL AERONAUTICS AND SPACE ADMINISTRATION • WASHINGTON, D. C. • APRIL 1966

NASA TN D-3171

SUPERSONIC FLUTTER OF SIMPLY SUPPORTED ISOTROPIC SANDWICH PANELS

By Larry L. Erickson and Melvin S. Anderson

Langley Research Center
Langley Station, Hampton, Va.

NATIONAL AERONAUTICS AND SPACE ADMINISTRATION

For sale by the Clearinghouse for Federal Scientific and Technical Information
Springfield, Virginia 22151 – Price $0.75

SUPERSONIC FLUTTER OF SIMPLY SUPPORTED ISOTROPIC SANDWICH PANELS*

By Larry L. Erickson and Melvin S. Anderson
Langley Research Center

SUMMARY

A theoretical solution using two-dimensional static aerodynamics is presented for the supersonic flutter characteristics of flat rectangular isotropic sandwich panels with simply supported edges. Tables and charts giving the values of the dynamic-pressure parameter required for flutter are presented for various values of panel length-width ratio, shear flexibility, and midplane stress. It is found that a decrease in transverse shear stiffness will usually lower the dynamic pressure required to induce flutter. However, for certain cases of midplane tension the opposite effect occurs. Panel mode shapes are also presented and a comparison is made of the two-mode Galerkin, the preflutter, and the exact flutter solutions.

INTRODUCTION

Panel flutter is an important design consideration for vehicles traveling at high Mach numbers. Consequently, considerable literature has been published dealing with several aspects of the problem. (See ref. 1.) One aspect which has not been adequately evaluated is the effect of transverse shear flexibility on the flutter characteristics of sandwich panels. Light-weight structural configurations for supersonic and hypersonic vehicles may incorporate stiffened panels such as honeycomb sandwich panels which in most cases cannot be considered rigid in shear. Therefore, unconservative designs may result if the transverse shear stiffness of such panels is not taken into account.

An estimate of the influence of shear flexibility on panel flutter was provided in reference 2 for flat and curved isotropic panels and in reference 3 for orthotropic panels where results of two-mode Galerkin solutions were presented. However, it is known that these approximate solutions become increasingly in error as the length-width ratio increases. As in references 2 and 3, it is assumed herein that the aerodynamic loading is given by two-dimensional static aerodynamics which are incorporated with the

*The basic theoretical development presented herein was given in a thesis by Melvin S. Anderson in partial fulfillment of the requirements for the degree of Doctor of Philosophy in Engineering Mechanics, Virginia Polytechnic Institute, Blacksburg, Virginia, June 1965.

small-deflection theory for flat sandwich panels developed in reference 4. However, in the present investigation, the resulting differential equations are solved exactly.

The results of reference 5 indicate that for the range of parameters shown therein, panel flutter analyses based on this simple aerodynamic theory are reasonably accurate for isotropic panels without shear flexibility when compared with the results obtained by using three-dimensional unsteady aerodynamics. Thus, for most cases, the results obtained herein are not expected to differ greatly from results that would be obtained by using more accurate aerodynamic theories.

The numerical results of the analysis are presented in the form of tables and charts and are discussed. Details of the analysis appear in the appendixes.

SYMBOLS

A,B,C coefficients appearing in equations (A6)

$\overline{A} = \frac{\eta^4}{\left(1 - rk_x\right)}\left[k_x - 2n^2 + r\left(n^2k_x + \phi\right)\right]$

a length of panel

$\overline{B} = \frac{\eta^4}{1 - rk_x}\left[\phi\left(1 + n^2r\right) - n^4\right]$

b width of panel

D flexural stiffness of isotropic sandwich panel, $\frac{E_f t_f h_c{}^2\left(1 + \frac{t_f}{h_c}\right)^2}{2\left(1 - \mu^2\right)} + \frac{E_f t_f{}^3}{6\left(1 - \mu^2\right)}$

D_Q transverse shear stiffness of isotropic sandwich panel, $G_c h_c\left(1 + \frac{t_f}{h_c}\right)^2$

D_1,D_2,D_3 coefficients defined by equations (A15)

E_f Young's modulus for faces of isotropic sandwich panel

$F(\ )$ function defined by equation (A25)

G_c shear modulus for core of isotropic sandwich panel

h_c depth of sandwich core

j,m,n integers

k_x, k'_x midplane stress parameters, $\frac{N_x b^2}{\pi^2 D}$, $\frac{N_x a^2}{\pi^2 D}$

l lateral aerodynamic loading

M free-stream Mach number

M_x, M_y intensity of internal bending moments acting upon a cross section originally parallel to the yz and xz planes, respectively

M_{xy} intensity of internal twisting moment acting in a cross section originally parallel to yz plane or xz plane

$\bar{m}$ exponent in equations (A6), denotes roots of equation (A9) when used with subscript j

N_x, N_y intensity of middle plane forces parallel to x and y axes, respectively (positive in compression)

$P = \frac{r}{1 + r}$

Q_x, Q_y intensity of internal shears acting in z-direction in cross sections originally parallel to yz and xz planes, respectively

q free-stream dynamic pressure, $\frac{1}{2}\rho_a V^2$

$R = \frac{r/\eta^2}{1 + r}$

r,r' shear flexibility parameters, $\frac{\pi^2 D}{b^2 D_Q}$, $\frac{\pi^2 D}{a^2 D_Q}$

S,T coefficients defined by equations (A30)

$s = P \cdot \frac{\overline{A}}{\eta^2}$

t time

t_f thickness of sandwich face plates

V free-stream velocity of airflow

w deflection of middle surface of plate, measured in z-direction

x,y,z orthogonal coordinates (see fig. 1)

α,δ,ϵ assumed components of roots of equation (A9) (See eqs. (A11))

$\beta = \sqrt{M^2 - 1}$

$\overline{\beta}_j = \frac{\overline{m}_j}{\pi\eta}$

Γ coefficient defined by equations (B6)

$\gamma = \frac{\lambda\eta r}{4\pi^2\left(1 - rk_x\right)}$

$\zeta = \gamma - \alpha$

η panel length-width ratio, $\frac{a}{b}$

λ,λ' dynamic pressure parameters, $\frac{2qb^3}{\beta D}$, $\frac{2qa^3}{\beta D}$

$\overline{\lambda} = \lambda\eta^3 \frac{1 + n^2 r}{1 - rk_x}$

μ Poisson's ratio for sandwich panel, defined in terms of curvatures

$\xi = \gamma + \alpha$

ρ_a free-stream mass density of air

ρ_m mass density per unit area of panel

ϕ,ϕ' frequency parameters, $\left(\frac{\omega}{\omega_r}\right)^2 + n^2 \frac{N_y b^2}{\pi^2 D}$ and $\left(\frac{\omega}{\omega_{r'}}\right)^2 + n^2 \frac{N_y a^2}{\pi^2 D}$

$$\frac{1}{\psi_j} = \left(\frac{1}{1 - \overline{\beta}_j^2}\right) + r$$

$\Omega = \tan^{-1} R$

ω panel frequency

ω_r, ω_r' fundamental frequency of simply supported panel rigid in shear with an infinite length or width, respectively, $\sqrt{\frac{\pi^4 D}{b^4 \rho_m}}, \sqrt{\frac{\pi^4 D}{a^4 \rho_m}}$

$[\ ]$ square matrix

$\{\ \}$ column matrix

Subscripts:

∞ evaluated at $\frac{a}{b} = \infty$

cr denotes flutter value of parameters

p denotes preflutter value

A comma followed by a subscript denotes differentiation with respect to the subscript.

THEORY AND ASSUMPTIONS

The configuration analyzed is shown in figure 1. It consists of a flat rectangular sandwich panel mounted on simple supports. The panel core and face materials are isotropic; hence, the panel itself is referred to as being isotropic. The panel has a length a and a width b and is subjected to uniform midplane force intensities N_x and N_y (positive in compression). The supersonic flow at Mach number M is over the top surface of the panel and is parallel to the x-axis.

The analysis of the configuration is based on the small deflection theory for flat sandwich panels developed in reference 4. This theory incorporates the effect of shear deformations by expressing the total panel curvature in the x- or y-direction and the twisting distortion as the sum of the contributions made by each of the internal

shears (Q_x, Q_y) and moments (M_x, M_y, M_{xy}). The resulting force-distortion equations can be solved for the three separate moments. Substitution of these expressions for the moments into the equations for equilibrium of moments about the x- and y-axes and the equation for equilibrium of vertical forces yields three independent equations relating the lateral displacement w and the two average shear angles Q_x/D_Q and Q_y/D_Q. These equations include the in-plane force intensities and the lateral loading. In the analysis presented herein, the lateral loading is comprised of the inertia force and the pressure due to supersonic flow (given by two-dimensional static aerodynamics). In-plane and rotary inertia loadings are not considered.

The boundary conditions imposed are those of simple supports, but inclusion of shear effects requires that a third boundary condition be satisfied in addition to the two usual conditions of zero moment and middle-surface deflection along the panel edges. This third boundary condition depends on the assumption made for the panel support. If the support is applied only to the middle surface of the panel, the boundary condition is that M_{xy} must vanish. If the support is assumed to be applied over the entire thickness of the panel the shear angle Q_x/D_Q is zero along an edge parallel to the x-axis because there is no x-displacement of points at the boundary. Similarly, the shear angle Q_y/D_Q is zero along an edge parallel to the y-axis. The last boundary condition (shear angle of 0^o) is usually the more closely approached in practice and is the one used herein. The exact solutions to the differential equations, subject to the stated boundary conditions, lead to a transcendental characteristic equation from which the panel frequencies and mode shapes can be determined as a function of midplane loads and dynamic pressure.

For the type of aerodynamic-force approximation used herein, flutter is known to occur only if variations of airflow or panel parameters can force a coalescence of two panel frequencies (ref. 6). The locus of such points forms a flutter boundary that separates a region of stable motion, where all frequencies are real and distinct, from a region of dynamic instability where at least one pair of frequencies are complex conjugates. Details of the exact solution together with a practical procedure for obtaining numerical flutter results are presented in appendix A.

RESULTS AND DISCUSSION

For a panel of given length or width, the flutter value of the dynamic pressure q is a function of the length-width ratio a/b, the bending and shear stiffnesses D and D_Q, respectively, and the in-plane load N_x. For the presentation of results, these variables are expressed in terms of nondimensional parameters.

Numerical results of the analysis are presented in tabular form in tables I and II. Table I is for $a/b < 1$, where flutter values of the dynamic-pressure parameter

$\lambda'_{cr} = \frac{2qa^3}{\beta D}$ and the frequency parameter $\phi'_{cr} = \frac{\rho_m a^4}{\pi^4 D}\omega^2 + \frac{a^2}{\pi^2 D}N_y$ are tabulated for various values of the shear-flexibility parameter $r' = \frac{\pi^2 D}{a^2 D_Q}$ and the stress parameter $k'_x = \frac{N_x a^2}{\pi^2 D}$. The flutter values λ'_{cr} were obtained by plotting frequency loops (λ' against ϕ', see fig. 2) for constant values of r', k'_x, and a/b. At the peak of the frequency loop $\lambda' = \lambda'_{cr}$ and any increase in λ' produces flutter. The flutter values of ϕ' associated with λ'_{cr} incorporate N_y and can be used to determine flutter frequencies ω_{cr}. As in the case for panels which are rigid in shear, the flutter value of q is not affected by N_y. Table II is for $\frac{a}{b} \geqq 1$ and to keep the numerical values of the tabulated results within reasonable size, the parameters have been redefined in terms of b. Thus, in table II, flutter values of $\lambda_{cr} = \frac{2qb^3}{\beta D}$ and $\phi_{cr} = \frac{\rho_m b^4}{\pi^4 D}\omega^2 + \frac{b^2}{\pi^2 D}N_y$ are tabulated for values of $r = \frac{\pi^2 D}{b^2 D_Q}$ and $k_x = \frac{N_x b^2}{\pi^2 D}$. Note that all results are presented in terms of the shorter dimension of the panel. Tables I and II also contain values of a parameter α which can be used to calculate flutter mode shapes. (See appendix A.) In table II, results are not presented for any value of a/b greater than that required to produce $\lambda_{cr} = 0$.

The results in tables I and II are presented graphically in figures 3 and 4. To keep these figures within reasonable size, $(\lambda')^{1/3}_{cr}$ is plotted against a/b when $0 \leqq a/b \leqq 1$ and $\lambda^{1/3}_{cr}$ is plotted against b/a when $1 \leqq a/b \leqq \infty$ for different values of the shear-flexibility parameters r', r. The flutter boundaries appearing in each individual figure correspond to different values of the stress parameters k'_x, k_x. Figure 4 is for stress-free panels with various values of r' and r. It shows that λ'_{cr} is essentially independent of the panel width for $a/b \leqq 1/4$ and that λ_{cr} is essentially independent of length for $a/b \geqq 10$. Figure 4 also illustrates that a significant reduction in λ_{cr} can be caused by shear flexibility when the panel carries no in-plane loads in the x-direction. It should be noted that for $r = 0$ ($D_Q = \infty$), the panel is rigid in shear and for this case the results agree with those of reference 6.

Effect of Shear Stiffness and Stress on Flutter Boundaries

Figure 5 illustrates the effect of shear stiffness on λ_{cr} for a square panel. For a compressive force in the flow direction ($k_x > 0$), the theory predicts that as the panel is made less stiff in shear (r increasing), λ_{cr} will decrease. The same result holds for the stress-free panel. However, when the panel is in tension ($k_x < 0$), there are cases when theory predicts that a panel which is flexible in shear ($r > 0$) will flutter at a higher value of λ_{cr} than a panel of the same geometry which is rigid in shear ($r = 0$).

For example, when $k_x = -4$, it is seen that after a slight initial decrease, λ_{cr} increases steadily as the panel becomes more flexible in shear. At $r = 2$, $\lambda_{cr} = 1230$ which is over one-third larger than the $r = 0$ value of λ_{cr}. That an increase in panel stiffness can lower λ_{cr} is an unexpected theoretical result. Whether such a physical phenomena does actually occur or whether the theory employed does not accurately represent the panel behavior under certain combinations of shear stiffness and tensile loading is not known. Consequently, such results should be regarded cautiously until refinements in the theory (for example, consideration of rotary inertia) or experimental evidence either confirm or refute this anomalous behavior.

The analysis presented in appendix A is based on the criteria that flutter occurs when two panel frequencies coalesce. Any circumstances that cause two in-vacuo frequencies to coincide will then produce, by this definition, flutter even though the dynamic pressure approaches zero. Inclusion of either aerodynamic or structural damping in theoretical flutter analyses of panels which are rigid in shear has been shown to remove these zero-dynamic-pressure flutter points (ref. 5); the resulting theoretical flutter boundaries, however, still do not compare well with experimental boundaries. Thus, to gain an idea of conditions for which the theoretical results can no longer be considered reliable, it is important to know the combinations of r, k_x, and a/b which produce zero-dynamic-pressure flutter points. These combinations can be determined from the in-vacuo vibration characteristics of the panel as described in appendix C. The primary results are shown in figure 6. When $k_x = \frac{2 + r}{(1 + r)^2}$, λ_{cr} approaches zero as a/b approaches infinity. If k_x is greater than $\frac{2 + r}{(1 + r)^2}$, then λ_{cr} goes to zero at values of a/b given by equation (C5) in appendix C. If k_x is less than $\frac{2 + r}{(1 + r)^2}$, then λ_{cr} never reaches zero but has a finite asymptotic value as a/b approaches infinity.

Comparison of Exact Results With Approximate Solutions

Modal solution.- Development of the exact solution provides an opportunity for evaluating the approximate two-mode Galerkin solution of reference 2. A comparison of flutter boundaries is shown in figure 7 for stress-free panels. Note that the two-mode solution becomes less accurate as r increases. Also, as in the $r = 0$ case, it becomes less accurate as a/b increases. At $a/b = \infty$, the two-mode solution predicts that $\lambda_{cr} = 0$.

An explanation for the growing inaccuracy of the two-mode solution with increasing shear flexibility is indicated by the exact flutter mode shapes for square stress-free panels shown in figure 8. (These shapes were calculated (from eq. (A29)) by using the values of α given in tables I and II.) As the panel becomes weaker in shear, the point of

maximum amplitude moves toward the trailing edge of the panel. Thus, it would be expected that the representation of the true mode shape by only two terms in a sine series, as was done in reference 2, would lead to increasingly inaccurate results as r increases.

Preflutter solution.- In reference 7, a solution to the differential equation of motion for simply supported panels that are rigid in shear was made and it yielded simple algebraic expressions for λ and ϕ. This solution corresponds to a point on the frequency loop which is not necessarily at the peak; thus, a value of λ is given which is less than or equal to λ_{cr}, hence the name "preflutter." When transverse shear effects are considered, it is found that a simple preflutter solution still exists (appendix B), even though two additional differential equations and an additional boundary condition must be satisfied.

As can be seen from figure 9, which is for stress-free panels, the preflutter solution gives values of λ that are very close to λ_{cr} when a/b is sufficiently large. For small values of a/b the preflutter solution is often in poor agreement with the exact solution. Its behavior is typical of that shown in figure 10 which is for $r = 2.0$. When $a/b = 1$, the preflutter solution corresponds to a point low on the second leg of the frequency loop. As a/b increases, this point moves along the second leg until at $a/b = 4$ it is nearly at the top of the frequency loop and is thus virtually identical with λ_{cr}. As a/b continues to increase, the preflutter point moves to the top of the loop (becoming exactly equal to λ_{cr}) and then starts down the first leg. Once on the first leg, however, it stays relatively close to the top of the loop, and thus gives a close approximation to λ_{cr}.

For increasingly large values of a/b, it becomes more difficult to obtain numerical results from the exact solution for λ_{cr}. Hence, it is desirable to be able to use the simpler preflutter solution in the range where it agrees closely with the exact solution. Table III shows a comparison of the preflutter solution with λ_{cr} at $a/b = 20$ for the values of r and k_x which are presented in table II. In all cases the solutions differ by less than 2 percent. Thus, the preflutter results used in table II and in figures 2 and 3 for $a/b > 20$ are justified as being good approximations to λ_{cr}.

CONCLUDING REMARKS

Charts have been presented to facilitate the determination of theoretical values of the dynamic pressure required to produce flutter of flat rectangular isotropic sandwich panels with simply supported edges. The flutter value of the dynamic pressure for a panel of given length or width is found to be a function of the length-width ratio, the bending and shear stiffnesses, and the in-plane load acting parallel to the airflow. It is independent of the in-plane load acting perpendicular to the airflow as long as buckling does not occur.

The theory predicts that a reduction in transverse shear stiffness usually causes a panel to be more susceptible to flutter. An unusual result is obtained for panels which carry tension loads in the direction parallel to the airflow. In these cases it is theoretically possible for a reduction in shear stiffness to make a panel less susceptible to flutter. However, this result should be regarded cautiously since at present there is no experimental evidence available with which to compare such theoretical behavior.

A comparison is made between the exact solution for the flutter dynamic pressure and two approximate solutions. A two-mode Galerkin solution is shown to become increasingly inaccurate as a panel becomes more flexible in shear. A relatively simple preflutter expression is found to give results that are in good agreement with the exact solution for sufficiently large length-width ratios.

Langley Research Center,
National Aeronautics and Space Administration,
Langley Station, Hampton, Va., November 8, 1965.

APPENDIX A

EXACT SOLUTION FOR THE SUPERSONIC FLUTTER BEHAVIOR OF SANDWICH PANELS

Differential Equations

The small-deflection equilibrium equations used herein to represent the behavior of a sandwich panel are derived in reference 4 by use of the following force-distortion equations which relate moments M_x, M_y, M_{xy}, shears Q_x, Q_y, and displacement w:

$$\left.\begin{aligned} M_x &= -D\left[\frac{\partial}{\partial x}\left(\frac{\partial w}{\partial x} - \frac{Q_x}{D_Q}\right) + \mu\frac{\partial}{\partial y}\left(\frac{\partial w}{\partial y} - \frac{Q_y}{D_Q}\right)\right] \\ M_y &= -D\left[\frac{\partial}{\partial y}\left(\frac{\partial w}{\partial y} - \frac{Q_y}{D_Q}\right) + \mu\frac{\partial}{\partial x}\left(\frac{\partial w}{\partial x} - \frac{Q_x}{D_Q}\right)\right] \\ M_{xy} &= \frac{1-\mu}{2}D\left[\frac{\partial}{\partial x}\left(\frac{\partial w}{\partial y} - \frac{Q_y}{D_Q}\right) + \frac{\partial}{\partial y}\left(\frac{\partial w}{\partial x} - \frac{Q_x}{D_Q}\right)\right] \end{aligned}\right\} \tag{A1}$$

where the bending and shear stiffnesses as given in reference 8 are

$$\left.\begin{aligned} D &= \frac{E_f t_f h_c^2\left(1 + \frac{t_f}{h_c}\right)^2}{2(1-\mu)^2} + \frac{E_f t_f^3}{6(1-\mu)^2} \\ D_Q &= G_c h_c\left(1 + \frac{t_f}{h_c}\right)^2 \end{aligned}\right\} \tag{A2}$$

respectively, and μ is Poisson's ratio. The assumptions involved in equations (A1) require that a straight line perpendicular to the undeformed middle surface of the panel remain straight and of constant length after deformation but not necessarily perpendicular to the deformed middle surface. This inclination in the x- (or y-) direction from a right angle is the average shear angle $\frac{Q_x}{D_Q}\left(\text{or } \frac{Q_y}{D_Q}\right)$.

The lateral aerodynamic pressure given by static linearized two-dimensional supersonic flow theory is

$$l = \frac{-2q}{\beta}\frac{\partial w}{\partial x} \tag{A3}$$

where $q = \frac{1}{2}\rho_a V^2$ is the free-steam value of the dynamic pressure and $\beta = \sqrt{M^2 - 1}$.

Substituting the above expression for l, together with the lateral inertia loading, into the three equilibrium equations of reference 4 yields

$$\left.\begin{aligned} &-N_x w_{,xx} - N_y w_{,yy} + Q_{x,x} + Q_{y,y} - \rho_m w_{,tt} - \frac{2q}{\beta} w_{,x} = 0 \\ &-w_{,xyy} - w_{,xxx} - \frac{Q_x}{D} + \frac{1}{D_Q}\left[Q_{x,xx} + \left(\frac{1-\mu}{2}\right)Q_{x,yy} + \left(\frac{1+\mu}{2}\right)Q_{y,xy}\right] = 0 \\ &-w_{,xxy} - w_{,yyy} - \frac{Q_y}{D} + \frac{1}{D_Q}\left[Q_{y,yy} + \left(\frac{1-\mu}{2}\right)Q_{y,xx} + \left(\frac{1+\mu}{2}\right)Q_{x,xy}\right] = 0 \end{aligned}\right\} \tag{A4}$$

where ρ_m is the mass per unit area of the panel and N_x and N_y are positive in compression.

Satisfaction of Boundary Conditions Along the Streamwise Edges

For the simply supported edges parallel to the x-axis at which the support is applied over the entire thickness, the boundary conditions are (see ref. 4)

$$\left.\begin{aligned} w &= 0 \\ M_y &= 0 \\ \frac{Q_x}{D_Q} &= 0 \end{aligned}\right\} \tag{A5}$$

General product solutions for the lateral deflection and the shears which satisfy these boundary conditions are

$$\left.\begin{aligned} w(x,y,t) &= Ae^{\bar{m}\frac{x}{a}} \sin n\pi \frac{y}{b} e^{i\omega t} \\ Q_x(x,y,t) &= Be^{\bar{m}\frac{x}{a}} \sin n\pi \frac{y}{b} e^{i\omega t} \\ Q_y(x,y,t) &= Ce^{\bar{m}\frac{x}{a}} \cos n\pi \frac{y}{b} e^{i\omega t} \end{aligned}\right\} \tag{A6}$$

where n is an integer indicating the number of sinusoidal half-waves in the y-direction and ω is the panel frequency. The expressions for w, Q_x, and Q_y also satisfy the differential equations (A4) provided that

APPENDIX A

$$\begin{bmatrix} \left(-k_x \frac{\bar{m}^2}{\pi^2} + \phi\eta^2 - \frac{\lambda\eta\bar{m}}{\pi^4}\right) & \frac{\bar{m}}{\pi} & -n \\ \frac{\bar{m}}{\pi}\left(n^2\eta^2 - \frac{\bar{m}^2}{\pi^2}\right) & -\eta^2 + r\frac{\bar{m}^2}{\pi^2} - \left(\frac{1-\mu}{2}\right)\eta^2 n^2 r & -\frac{\bar{m}}{\pi}\left(\frac{1+\mu}{2}\right)nr \\ n\left(n^2\eta^2 - \frac{\bar{m}^2}{\pi^2}\right) & \frac{\bar{m}}{\pi}\left(\frac{1+\mu}{2}\right)nr & -\left(1 + n^2 r\right) + \left(\frac{1-\mu}{2}\right)\frac{r}{\eta^2}\frac{\bar{m}^2}{\pi^2} \end{bmatrix} \begin{Bmatrix} A \\ \frac{ab^2}{\pi^3 D}B \\ \frac{a^2 b}{\pi^3 D}C \end{Bmatrix} = \begin{Bmatrix} 0 \\ 0 \\ 0 \end{Bmatrix} \tag{A7}$$

where

$$\left.\begin{aligned} \eta &= \frac{a}{b} \\ k_x &= \frac{N_x b^2}{\pi^2 D} \\ r &= \frac{\pi^2 D}{b^2 D_Q} \\ \lambda &= \frac{2qb^3}{\beta D} \\ \phi &= \left(\frac{\omega}{\omega_r}\right)^2 + n^2\frac{N_y b^2}{\pi^2 D} \\ \omega_r^2 &= \frac{\pi^4 D}{b^4 \rho_m} \end{aligned}\right\} \tag{A8}$$

Nontrivial solutions are obtained by equating the determinant of the matrix in equation (A7) to zero. Expanding this determinant leads to

$$\left(\bar{m}^4 - 4\gamma\bar{m}^3 + \pi^2\bar{A}\bar{m}^2 + \bar{\lambda}\bar{m} - \pi^4\bar{B}\right)\left[1 - \frac{n^2 r}{\eta^2}\left(\frac{1-\mu}{2}\right)\left(\frac{\bar{m}^2}{\pi^2 n^2} - \eta^2\right)\right] = 0 \tag{A9}$$

where

$$\left.\begin{aligned}
\gamma &= \frac{\lambda\eta r}{4\pi^2(1 - rk_x)} \\
\overline{A} &= \frac{\eta^2}{1 - rk_x}\left[k_x - 2n^2 + r\left(n^2k_x + \phi\right)\right] \\
\overline{\lambda} &= \lambda\eta^3\frac{1 + n^2r}{1 - rk_x} \\
\overline{B} &= \frac{\eta^4}{1 - rk_x}\left[\phi(1 + n^2r) - n^4\right]
\end{aligned}\right\} \tag{A10}$$

If the roots of equation (A9) are written in a form similar to that used in reference 6,

$$\left.\begin{aligned}
\overline{m}_1 &= \gamma + \alpha + i\delta \\
\overline{m}_2 &= \gamma + \alpha - i\delta \\
\overline{m}_3 &= \gamma - \alpha + \epsilon \\
\overline{m}_4 &= \gamma - \alpha - \epsilon \\
\overline{m}_5 &= \pi\eta n\left[1 + \frac{2}{(1 - \mu)n^2r}\right]^{1/2} \\
\overline{m}_6 &= -\overline{m}_5
\end{aligned}\right\} \tag{A11}$$

they can be related to the coefficients in equation (A9) as follows:

$$6\gamma^2 - 2\alpha^2 + \delta^2 - \epsilon^2 = \pi^2\overline{A} \tag{A12a}$$

$$2\alpha\left(\delta^2 + \epsilon^2\right) - 2\gamma\left[\delta^2 - \epsilon^2 + 2\left(\gamma^2 - \alpha^2\right)\right] = \bar{\lambda} \tag{A12b}$$

$$\gamma^4 + \gamma^2\left(\delta^2 - \epsilon^2 - 2\alpha^2\right) - 2\alpha\gamma\left(\epsilon^2 + \delta^2\right) + \left(\alpha^2 - \epsilon^2\right)\left(\alpha^2 + \delta^2\right) = -\pi^4\bar{B} \tag{A12c}$$

For computational purposes it is convenient to solve equations (A12a) and (A12b) for δ and ϵ.

$$\left.\begin{aligned} \delta^2 &= \frac{\bar{\lambda}}{4\alpha} + \alpha^2 + \frac{\pi^2\bar{A}}{2} - \frac{\gamma}{\alpha}\left(2\gamma^2 + 3\gamma\alpha - \pi^2\frac{\bar{A}}{2}\right) \\ \epsilon^2 &= \frac{\bar{\lambda}}{4\alpha} - \alpha^2 - \frac{\pi^2\bar{A}}{2} - \frac{\gamma}{\alpha}\left(2\gamma^2 - 3\gamma\alpha - \pi^2\frac{\bar{A}}{2}\right) \end{aligned}\right\} \tag{A13}$$

It should be noted that δ^2 and ϵ^2 could be negative and this possibility was allowed for in the calculations by taking into account any imaginary quantities that appear. However, for the ranges of parameters covered in the calculations, δ was real for any point on the frequency loop and ϵ was real except at sufficiently high axial compression where ϵ became imaginary. Using these relations to eliminate δ and ϵ from equation (A12c) yields the following cubic in α^2

$$\alpha^6 - D_1\alpha^4 + D_2\alpha^2 - D_3 = 0 \tag{A14}$$

where

$$\left.\begin{aligned} D_1 &= 3\gamma^2 - \frac{\pi^2\bar{A}}{2} \\ D_2 &= \left(2\gamma^2 - \frac{\pi^2\bar{A}}{4}\right)^2 + \frac{1}{4}\left(\pi^4\bar{B} - \gamma\bar{\lambda}\right) - \gamma^4 \\ D_3 &= \left[\frac{\bar{\lambda}}{8} - \gamma\left(\gamma^2 - \frac{\pi^2\bar{A}}{4}\right)\right]^2 \end{aligned}\right\} \tag{A15}$$

Equations (A13) and (A14) provide a procedure for obtaining numerical values of λ once the boundary conditions at $x = 0$ and $x = a$ are satisfied.

APPENDIX A

Satisfaction of Boundary Conditions Along the Leading and Trailing Edges

For the simply supported edges parallel to the y-axis at which the support is applied over the entire thickness, the boundary conditions are the same as those given by equations (A5) if y and x are interchanged. Before the boundary conditions can be applied to the solutions given by equations (A6), it is necessary to express w, Q_x, and Q_y in terms of one set of coefficients (that is, either A, B, or C). The coefficient A can be eliminated from the second and third rows of matrix equation (A7). The result is

$$\left[1 - \frac{n^2 r}{\eta^2}\left(\frac{1-\mu}{2}\right)\left(\frac{\overline{m}_j^2}{n^2\pi^2} - \eta^2\right)\right]\left[\eta B_j - \frac{\overline{m}_j}{n\pi} C_j\right] = 0 \tag{A16}$$

When j equals 5 or 6, the first bracketed term is equal to zero (eqs. (A9) and (A11)) and no information is obtained about the relationship between B_j and C_j. However, when $j = 1, 2, 3, 4$, the first bracketed term is not, in general, equal to zero. Therefore,

$$C_j = \frac{\pi\eta n}{\overline{m}_j} B_j \qquad (j = 1, 2, 3, 4) \tag{A17}$$

Replacing C_j with $\frac{\pi\eta n}{\overline{m}_j} B_j$ in the third row of equation (A7) gives

$$A_j = \left[\frac{\pi^2\eta^2 + r\left(\pi^2 n^2 \eta^2 - \overline{m}_j^2\right)}{\overline{m}_j \pi^2 \left(\pi^2 n^2 \eta^2 - \overline{m}_j^2\right)}\right] \frac{ab^2}{D} \cdot B_j \qquad (j = 1, 2, 3, 4) \tag{A18}$$

If C_j is eliminated from the first and second of equations (A7), it is found that

$$A_j\left\{\left[-k_x \frac{\overline{m}_j^2}{\pi^2} + \phi\eta^2 - \frac{\lambda\eta\overline{m}_j}{\pi^4}\right]\left(\frac{1+\mu}{2}\right)\frac{\overline{m}_j r}{\pi} + \frac{\overline{m}_j}{\pi}\left(\frac{\overline{m}_j^2}{\pi^2} - n^2\eta^2\right)\right\} = \frac{-a^3}{\pi^3 D}\left[1 - \frac{n^2 r}{\eta^2}\left(\frac{1-\mu}{2}\right)\left(\frac{\overline{m}_j^2}{n^2\pi^2} - \eta^2\right)\right] B_j \tag{A19}$$

Again, the bracketed term before B_j is zero for j equal to 5 or 6. The coefficient of A_j is not, in general, equal to zero and therefore

$$A_5 = A_6 = 0 \tag{A20}$$

Thus, for j equal to 5 and 6, the first of equation (A7) gives

$$C_j = \frac{\overline{m}_j}{n\eta\pi} B_j \tag{A21}$$

Use of these relations enables equations (A6) to be written in terms of B_j alone as follows:

$$\left.\begin{aligned} w &= \sum_{j=1}^{4}\left[\frac{\pi^2\eta^2 + r\left(\pi^2 n^2\eta^2 - \bar{m}_j^2\right)}{\bar{m}_j\pi^2\left(\pi^2 n^2\eta^2 - \bar{m}_j^2\right)}\right]\frac{ab^2}{D}B_j e^{\bar{m}_j\frac{x}{a}}\sin n\pi\frac{y}{b}e^{i\omega t} \\ Q_x &= \sum_{j=1}^{6} B_j e^{\bar{m}_j\frac{x}{a}}\sin n\pi\frac{y}{b}e^{i\omega t} \\ Q_y &= \left[\sum_{j=1}^{4}\frac{\pi n\eta}{\bar{m}_j}B_j e^{\bar{m}_j\frac{x}{a}} + \sum_{j=5}^{6}\frac{\bar{m}_j}{\pi n\eta}B_j e^{\bar{m}_j\frac{x}{a}}\right]\cos n\pi\frac{y}{b}e^{i\omega t} \end{aligned}\right\} \qquad \text{(A22)}$$

Substituting the above expressions for w, Q_x, and Q_y into the boundary condition equations yields

$$\begin{bmatrix} \left(\frac{1}{n^2-\bar{\beta}_1^3}+r\right)\frac{1}{\bar{\beta}_1} & \left(\frac{1}{n^2-\bar{\beta}_2^2}+r\right)\frac{1}{\bar{\beta}_2} & \left(\frac{1}{n^2-\bar{\beta}_3^2}+r\right)\frac{1}{\bar{\beta}_3} & \left(\frac{1}{n^2-\bar{\beta}_4^2}+r\right)\frac{1}{\bar{\beta}_4} & 0 & 0 \\ \left(\frac{1}{n^2-\bar{\beta}_1^2}+r\right)\frac{e^{\bar{m}_1}}{\bar{\beta}_1} & \left(\frac{1}{n^2-\bar{\beta}_2^2}+r\right)\frac{e^{\bar{m}_2}}{\bar{\beta}_2} & \left(\frac{1}{n^2-\bar{\beta}_3^2}+r\right)\frac{e^{\bar{m}_3}}{\bar{\beta}_3} & \left(\frac{1}{n^2-\bar{\beta}_4^2}+r\right)\frac{e^{\bar{m}_4}}{\bar{\beta}_4} & 0 & 0 \\ \frac{-\bar{\beta}_1}{n^2-\bar{\beta}_1^2} & \frac{-\bar{\beta}_2}{n^2-\bar{\beta}_2^2} & \frac{-\bar{\beta}_3}{n^2-\bar{\beta}_3^2} & \frac{-\bar{\beta}_4}{n^2-\bar{\beta}_4^2} & r\bar{\beta}_5 & r\bar{\beta}_6 \\ \frac{-\bar{\beta}_1 e^{\bar{m}_1}}{n^2-\bar{\beta}_1^2} & \frac{-\bar{\beta}_2 e^{\bar{m}_2}}{n^2-\bar{\beta}_2^2} & \frac{-\bar{\beta}_3 e^{\bar{m}_3}}{n^2-\bar{\beta}_3^2} & \frac{-\bar{\beta}_4 e^{\bar{m}_4}}{n^2-\bar{\beta}_4^2} & r\bar{\beta}_5 e^{\bar{m}_5} & r\bar{\beta}_6 e^{\bar{m}_6} \\ \frac{n}{\bar{\beta}_1} & \frac{n}{\bar{\beta}_2} & \frac{n}{\bar{\beta}_3} & \frac{n}{\bar{\beta}_4} & \frac{\bar{\beta}_5}{n} & \frac{\bar{\beta}_6}{n} \\ \frac{n}{\bar{\beta}_1}e^{\bar{m}_1} & \frac{n}{\bar{\beta}_2}e^{\bar{m}_2} & \frac{n}{\bar{\beta}_3}e^{\bar{m}_3} & \frac{n}{\bar{\beta}_4}e^{\bar{m}_4} & \frac{\bar{\beta}_5 e^{\bar{m}_5}}{n} & \frac{\bar{\beta}_6 e^{\bar{m}_6}}{n} \end{bmatrix}\begin{Bmatrix} B_1 \\ B_2 \\ B_3 \\ B_4 \\ B_5 \\ B_6 \end{Bmatrix} = \begin{Bmatrix} 0 \\ 0 \\ 0 \\ 0 \\ 0 \\ 0 \end{Bmatrix} \qquad \text{(A23)}$$

where $\bar{\beta}_j = \frac{\bar{m}_j}{\pi\eta}$.

The nontrivial solution for the deflected shape of the panel is obtained by equating the determinant of this matrix to zero. By manipulating rows and columns, additional zeroes can be introduced into columns 5 and 6 of this determinant so that it becomes

$$\begin{vmatrix} 1 & 1 & 1 & 1 \\ e^{\overline{m}_1} & e^{\overline{m}_2} & e^{\overline{m}_3} & e^{\overline{m}_4} \\ \overline{m}_1^2 & \overline{m}_2^2 & \overline{m}_3^2 & \overline{m}_4^2 \\ \overline{m}_1^2 e^{\overline{m}_1} & \overline{m}_2^2 e^{\overline{m}_2} & \overline{m}_3^2 e^{\overline{m}_3} & \overline{m}_4^2 e^{\overline{m}_4} \end{vmatrix} = 0 \qquad \text{(A24)}$$

Note that equation (A24) is independent of the roots $\overline{m}_5$ and $\overline{m}_6$. It is mathematically the same as for a panel which is rigid in shear except that the roots $\overline{m}_j$ are functions of the shear stiffness. (See eqs. (A11), (A10), and (A8).) Expanding equation (A24) and replacing the roots m_j with the expressions given by equations (A11) yields.

$$F(\alpha,\delta,\epsilon,\gamma) = \left[\left(\delta^2 + \epsilon^2\right)^2 + 4\alpha^2\left(\delta^2 - \epsilon^2\right) + 4\gamma^2\left(4\alpha^2 + \delta^2 - \epsilon^2\right)\right] \sin\delta \sinh\epsilon$$
$$-8\delta\epsilon\left(\alpha^2 - \gamma^2\right)\left(\cosh\epsilon \cos\delta - \cosh 2\alpha\right) = 0 \qquad \text{(A25)}$$

Equation (A25) reduces to equation (9) of reference 6 when γ equals zero (infinite transverse shear stiffness).

Relations (A10), (A13), (A14), and (A25) are 8 independent equations involving 13 quantities (r, k_x, η, ϕ, n, λ, $\overline{\lambda}$, $\overline{A}$, $\overline{B}$, γ, α, δ, ϵ). For simple supports these equations constitute the solution to equations (A4) once 5 of the 13 quantities are specified.

The differences between the results of the analysis presented herein and the results of reference 6 are due to the parameter r. In figure 11, some of these differences are illustrated by showing the relation between the frequency loops and the functions $\overline{A}$ and $\overline{B}$ which are defined by equations (A10). Regardless of r, λ reaches the value λ_{cr} when two of the frequencies of the panel coalesce. An increase in λ above λ_{cr} causes ω^2 to become complex. Thus, one of the two square roots of ω^2 must possess a negative imaginary part which by equation (A6) is associated with divergent motion or flutter.

When r is zero (infinite shear stiffness), the expressions for $\overline{A}$ and $\overline{B}$ reduce to the definitions in reference 6. In this case $\overline{A}$ is not a function of the frequency parameter ϕ and depends only on n, η, and k_x. The frequency loops (variation of λ with ϕ) then lie in planes of constant $\overline{A}$ and λ_{cr} is a function of $\overline{A}$ only. Hence, differing panel configurations with the same value of $\overline{A}$ but with different combinations of η and k_x will all theoretically flutter at an identical value of λ_{cr}. For r greater

than zero (finite shear stiffness), $\overline{A}$ is no longer independent of ϕ. As a result, the frequency loops are rotated out of the constant $\overline{A}$ planes by the angle

$$\Omega = \tan^{-1}\frac{r/\eta^2}{1+r} \tag{A26}$$

In this case n, η, and k_x do not form a single parameter determining λ_{cr}.

Two additional effects of nonzero r can be seen from figure 11. One of these is that the frequency loop tends to bend over in the direction of increasing frequency. As r increases, this effect becomes more pronounced. The second feature is that for $\lambda = 0$ (no airflow), the natural frequencies of the panel are reduced in magnitude as r is increased.

Procedure for Obtaining Numerical Values From Exact Solution

Since the flutter value of λ is sought for a given panel configuration and midplane stress condition, it is desirable to specify r, k_x, and η. If n and the frequency parameter ϕ are then prescribed, the remaining eight quantities can be determined. This process enables one to obtain the variation of λ with ϕ for fixed values of the length-width ratio and stress and shear-flexibility parameters.

A practical procedure for obtaining flutter values of λ for selected values of r, k_x, η, and n is as follows:

(1) Select ϕ, a good choice being a value midway between the first and second in-vacuo values of ϕ (see appendix C).

(2) Calculate $\overline{A}$ and $\overline{B}$ from equations (A10).

(3) Make an initial estimate for the correct value of $\overline{\lambda}$. Calculate corresponding values of λ and γ from equations (A10).

(4) Solve equation (A14) for α^2. The Newton-Raphson technique works very well since only one real root of equation (A14) was found to exist when the estimated value of $\overline{\lambda}$ was close to the correct value.

(5) Calculate δ and ϵ from equations (A13).

(6) Use equation (A25) to calculate $F(\alpha,\delta,\epsilon,\gamma)$, a nonzero value meaning an incorrect choice of $\overline{\lambda}$.

(7) Repeat steps 3 to 6 until a value of $\overline{\lambda}$ is found that differs from the correct value [that is, $F(\alpha,\delta,\epsilon,\gamma) = 0$] by only an acceptable amount. (An allowable error in λ of 0.01 percent was used in calculating the results presented herein.)

(8) Increase ϕ and repeat the process until the point $\frac{\partial\lambda}{\partial\phi} = 0$ is obtained.

When the numerical results presented in this report were obtained, the increments in ϕ were taken small enough to assure that the values of λ_{cr} were in error by no more than 1 percent. In most cases they are correct to 0.1 percent. In all cases, calculations show that the critical flutter solution is obtained by setting $n = 1$ and determining λ_{cr} from the coalescence of the two lowest frequencies.

Panel Mode Shape

The lateral deflection can be obtained from the first of equations (A6) once the coefficients A_j are known. These coefficients can be determined from equation (A23). If, in equation (A23), n is set equal to 1 and rows 5 and 6 are multiplied by r, and row 5 is subtracted from row 3 and row 6 is subtracted from row 4, the coefficients of B_5 and B_6 appearing in rows 3 and 4 can be made equal to zero. Then, replacing B_j with $\frac{\pi^3 D}{b^3}\psi_j\bar{\beta}_j A_j$ for $j = 1, 2, 3$, or 4, where

$$\psi_j = \left(\frac{1}{1 - \bar{\beta}_j^2} + r\right)^{-1} \tag{A27}$$

and recalling that $A_5 = A_6 = 0$ yields

$$\begin{bmatrix} 1 & 1 & 1 & 1 \\ e^{\bar{m}_1} & e^{\bar{m}_2} & e^{\bar{m}_3} & e^{\bar{m}_4} \\ \psi_1 & \psi_2 & \psi_3 & \psi_4 \\ \psi_1 e^{\bar{m}_1} & \psi_2 e^{\bar{m}_2} & \psi_3 e^{\bar{m}_3} & \psi_4 e^{\bar{m}_4} \end{bmatrix} \begin{Bmatrix} A_1 \\ A_2 \\ A_3 \\ A_4 \end{Bmatrix} = \begin{Bmatrix} 0 \\ 0 \\ 0 \\ 0 \end{Bmatrix} \tag{A28}$$

By a corrollary to Cramer's rule (ref. 9), the coefficients A_j can now be determined within an arbitrary constant. Substituting the expressions for A_j and the expressions for $\bar{m}_j$ given by equations (A11) into equation (A6) and ignoring the arbitrary constant yields, after considerable manipulation,

APPENDIX A

$$w\left(\frac{x}{a}\right) = \left[-Te^{\zeta}\sinh\epsilon + (\psi_3 - \psi_4)e^{\xi}\sin\delta\right]\left[e^{\xi\frac{x}{a}}\cos\delta\frac{x}{a} - e^{\zeta\frac{x}{a}}\cosh\epsilon\frac{x}{a}\right]$$

$$+\left[Se^{\zeta}\sinh\epsilon + (\psi_3 - \psi_4)e^{\xi}\cos\delta + \psi_3 e^{\zeta-\epsilon} - \psi_4 e^{\zeta+\epsilon}\right]e^{\xi\frac{x}{a}}\sin\delta\frac{x}{a}$$

$$+\left[-Te^{\zeta}\cosh\epsilon + (\psi_3 + \psi_4)e^{\xi}\sin\delta + e^{\xi}(T\cos\delta - S\sin\delta)\right]e^{\zeta\frac{x}{a}}\sinh\epsilon\frac{x}{a} \qquad \text{(A29)}$$

where

$$\left.\begin{aligned}
\xi &= \gamma + \alpha \\
\zeta &= \gamma - \alpha \\
\psi_3 &= \left[\frac{1}{1 - \left(\frac{\zeta + \epsilon}{\pi\eta}\right)^2} + r\right]^{-1} \\
\psi_4 &= \left[\frac{1}{1 - \left(\frac{\zeta - \epsilon}{\pi\eta}\right)^2} + r\right]^{-1} \\
\frac{S}{2} &= \frac{(1 + r)\pi^4\eta^4 + r\left(\xi^2 + \delta^2\right)^2 - \pi^2\eta^2(1 + 2r)\left(\xi^2 - \delta^2\right)}{(1 + r)^2\pi^4\eta^4 + r^2\left(\xi^2 + \delta^2\right)^2 - 2\pi^2\eta^2 r(1 + r)\left(\xi^2 - \delta^2\right)} \\
T &= \frac{-4\pi^2\eta^2\xi\delta}{(1 + r)^2\pi^4\eta^4 + r^2\left(\xi^2 + \delta^2\right)^2 - 2\pi^2\eta^2 r(1 + r)\left(\xi^2 - \delta^2\right)}
\end{aligned}\right\} \qquad \text{(A30)}$$

The flutter mode shapes for w presented in figure 8 were obtained from equation (A29) by using the values of α_{cr} in tables I and II.

APPENDIX B

PREFLUTTER SOLUTION

From equation (A25) it is seen that the transcendental equation $F(\alpha,\delta,\epsilon,\gamma) = 0$ is satisfied identically when $\epsilon = 2\alpha$ and $\delta = 2m\pi$ where m is an integer. (This same relationship was noticed in reference 7 for panels which are rigid in shear, and leads to the so-called "preflutter" solution.) Substituting these expressions for ϵ and δ into equations (A12) and setting $m = 1$ yields the following expression for $\overline{\lambda}$

$$\frac{\overline{\lambda}}{\pi^3} = \frac{4}{3}\left[10 - \overline{A} + 6\left(\frac{\gamma}{\pi}\right)^2\right]\sqrt{\frac{4 - \overline{A}}{6} + \left(\frac{\gamma}{\pi}\right)^2} - 2\left(\frac{\gamma}{\pi}\right)\overline{A} + 8\left(\frac{\gamma}{\pi}\right)^3 \tag{B1}$$

(Setting $m = 1$ restricts the preflutter solution to a point on the first frequency loop.) If the panel is rigid in shear ($r = \gamma = 0$), the following preflutter equations for λ and $\overline{B}$ are obtained

$$\left.\begin{aligned} \lambda &= \frac{4}{3}\left(\frac{\pi}{\eta}\right)^3\left(10 - \overline{A}\right)\sqrt{\frac{4 - \overline{A}}{6}} \\ \overline{B} &= \frac{4}{3}\left(7 - 2\overline{A}\right) + \frac{\overline{A}^2}{12} \end{aligned}\right\} \tag{B2}$$

where $\overline{A} = \eta^2(k_x - 2)$ is now independent of the panel frequency. As noted in reference 5, the first of equations (B2) yields values of λ that are very close to λ_{cr} when $\overline{A}$ is negative. (See fig. 9.)

For $r \neq 0$, preflutter values of λ are not so easily obtained since it is not possible to solve for λ as an explicit function of r, η, and k_x. However, it is possible to write equation (B1) in terms of r, η, and $\overline{A}$ by replacing $\frac{\gamma}{\pi}$ with $\frac{\overline{\lambda}}{4\pi^3}\left(\frac{r/\eta^2}{1 + r}\right)$. (See eqs. (A10).) The result is

$$\left(\frac{\overline{\lambda}}{\pi^3}\right)^2 = \frac{\left[1 + R\overline{A} - R^2\frac{\left(\overline{A} - 60\right)\left(\overline{A} - 4\right)}{12}\right] \pm \sqrt{\left[1 + R\overline{A} - R^2\frac{\left(\overline{A} - 60\right)\left(\overline{A} - 4\right)}{12}\right]^2 - \left(\frac{2}{3}R\right)^3(1 + 4R)\left(10 - \overline{A}\right)^2\left(4 - \overline{A}\right)}}{\frac{R^3}{2}(1 + 4R)} \tag{B3}$$

where

$$R = \frac{r/\eta^2}{1 + r}$$

Thus, if r, η, and $\overline{A}$ are specified, $\overline{\lambda}$ can be calculated. (Note that $\overline{A}$ is a function of the unknown frequency parameter ϕ.) Since $\overline{\lambda}$ is known, $\frac{\gamma}{\pi}$ can be determined from equations (A10); and then $\frac{\alpha}{\pi}$ and $\overline{B}$ can be obtained from equations (A12). The stress parameter k_x is obtained by eliminating ϕ from the expressions for $\overline{A}$ and $\overline{B}$ given by equations (A10):

$$k_x = \frac{\eta^2 \frac{2 + r}{1 + r} + \left(\overline{A} - R\overline{B}\right)}{\eta^2(1 + r) + r\left(\overline{A} - R\overline{B}\right)} \tag{B4}$$

Finally, λ is determined from the third of equations (A10). It should be noted that for fixed r and η, k_x cannot be specified arbitrarily since it is determined by the choice of $\overline{A}$ used in equation (B3). Thus, trial-and-error calculations involving different choices of $\overline{A}$ are necessary to obtain λ for the k_x of interest.

The preceding preflutter equations can be used for infinitely long panels by letting η approach ∞. This condition leads to the following expressions for λ and k_x:

$$\left.\begin{aligned} \lambda &= \sqrt{2}\pi^3 \Gamma \frac{1 - rk_x}{1 + r} \\ k_x &= \frac{\frac{2 + r}{1 + r} + \left[\left(\frac{\overline{A}}{\eta^2}\right) - P\left(\frac{\overline{B}}{\eta^4}\right)_\infty\right]}{1 + r + r\left[\left(\frac{\overline{A}}{\eta^2}\right) - P\left(\frac{\overline{B}}{\eta^4}\right)_\infty\right]} \end{aligned}\right\} \tag{B5}$$

where

$$\left.\begin{aligned}
\left(\frac{B}{\eta^4}\right)_\infty &= \frac{(P\Gamma)^4}{8} - \frac{(P\Gamma)^2}{4}\left(\frac{\bar{A}}{\eta^2}\right) + 2\sqrt{2}(P\Gamma)\left[\frac{(P\Gamma)^2}{8} - \frac{1}{6}\left(\frac{\bar{A}}{\eta^2}\right)\right]^{3/2} + \frac{1}{12}\left(\frac{\bar{A}}{\eta^2}\right)^2 \\
\Gamma &= \left(\frac{\bar{\lambda}^2}{2\eta^6\pi^6}\right)_\infty = \frac{(12 + 12s - s^2) \pm \sqrt{144 + 288s + 120s^2 + \frac{56}{3}s^3 + s^4}}{12P^3} \\
P &= \frac{r}{1 + r} \\
s &= P\frac{\bar{A}}{\eta^2}
\end{aligned}\right\} \qquad \text{(B6)}$$

Thus, by specifying r and $\frac{\bar{A}}{\eta^2}$, λ and k_x can be calculated for $\eta = \infty$.

An interesting solution occurs when $\frac{\bar{A}}{\eta^2} = 0$. If the negative root is used to calculate Γ, $\Gamma = \left(\frac{\bar{B}}{\eta^4}\right)_\infty = 0$. Hence,

$$\left.\begin{aligned}
k_x &= \frac{2 + r}{(1 + r)^2} \\
\lambda &= 0
\end{aligned}\right\} \qquad \text{(B7)}$$

That is, as k_x is increased to the value $\frac{2 + r}{(1 + r)^2}$, the preflutter value of λ for an infinitely long panel drops to zero. It is shown in appendix C that λ_{cr} also goes to zero as k_x approaches $\frac{2 + r}{(1 + r)^2}$ when $\eta = \infty$.

APPENDIX C

PANEL BEHAVIOR FOR ZERO DYNAMIC PRESSURE

The natural vibration characteristics of the panel can be obtained for zero dynamic pressure by setting $\lambda = \overline{\lambda} = \gamma = 0$. Then by equation (A14), α is also equal to zero. Equation (A25) reduces to $(\epsilon^2 + \delta^2)^2 \sin \delta \sinh \epsilon = 0$ so that

$$\delta = m\pi \tag{C1}$$

where m is an integer designating the number of sinusoidal half-waves in the x-direction. From equations (A12) and (C1), it is readily verified that $\epsilon^2 = \frac{\pi^2 \overline{B}}{m^2}$ and

$$B = m^2(m^2 - \overline{A}) \tag{C2}$$

Equations (C2) and (A10) lead to

$$\phi = \frac{\left[\left(\frac{m}{\eta}\right)^2 + n^2\right]^2}{1 + r\left[\left(\frac{m}{\eta}\right)^2 + n^2\right]} - \left(\frac{m}{\eta}\right)^2 k_x \tag{C3}$$

Use of the expression for ϕ as given by equation (A8) enables the in-vacuo natural frequencies to be expressed as

$$\left(\frac{\omega}{\omega_r}\right)^2 = \frac{\left[\left(\frac{m}{\eta}\right)^2 + n^2\right]^2}{1 + r\left[\left(\frac{m}{\eta}\right)^2 + n^2\right]} - \left[\left(\frac{m}{\eta}\right)^2 + n^2 \frac{N_y}{N_x}\right] k_x \tag{C4}$$

Equation (C4) can be used to calculate the in-vacuo buckling loads by equating the frequency to zero.

In the analysis presented in appendix A, it is assumed that flutter occurs when two frequencies of the panel coalesce or become equal. For certain values of the stress parameter k_x, two of the panel's in-vacuo natural frequencies become equal. This condition occurs whenever two consecutive mode lines cross one another as in figure 11 (that is, eq. (C2) is satisfied by two consecutive integer values of m). The numerical calculations which were made indicate that $\lambda_{cr} = 0$ at these points; that is, the frequency

loop degenerates to a point. The combinations of r, k_x, and η which produce these theoretical zero-dynamic-pressure flutter points can be determined by using equation (C3) to eliminate ϕ from the expression for $\overline{B}$ given by the last of equations (A10). Using the in-vacuo relation between $\overline{B}$ and $\overline{A}$ (eq. (C2)) then leads to

$$\eta^4\left[k_x - \frac{2 + r}{(1 + r)^2}\right] - \eta^2\left(\overline{A}\frac{1 - rk_x}{1 + r}\right) + r\overline{B}\frac{1 - rk_x}{1 + r} = 0 \tag{C5}$$

This equation gives the zero-dynamic-pressure flutter points in terms of r, k_x, and η. The values of $\overline{A}$ and $\overline{B}$ to be used are those for which equation (C2) is satisfied by two consecutive integer values of m. (The first zero-dynamic-pressure flutter point occurs at $\overline{A} = 5$.) (See fig. 6.)

REFERENCES

1. Fung, Y. C.: Some Recent Contributions to Panel Flutter Research. AIAA J., vol. 1, no. 4, Apr. 1963, pp. 898-909.

2. McElman, John A.: Flutter of Curved and Flat Sandwich Panels Subjected to Supersonic Flow. NASA TN D-2192, 1964.

3. Weidman, Deene J.: Effects of Side-Edge Boundary Conditions and Transverse Shear Stiffnesses on the Flutter of Orthotropic Panels in Supersonic Flow. NASA TN D-3302, 1966.

4. Libove, Charles; and Batdorf, S. B.: A General Small-Deflection Theory for Flat Sandwich Plates. NACA Rept. 899, 1948. (Supersedes NACA TN 1526.)

5. Bohon, Herman L.; and Dixon, Sidney C.: Some Recent Developments in Flutter of Flat Panels. J. Aircraft, vol. 1, no. 5, Sept.-Oct. 1964, pp. 280-288.

6. Hedgepeth, John M.: Flutter of Rectangular Simply Supported Panels at High Supersonic Speeds. J. Aeron. Sci., vol. 24, no. 8, Aug. 1957, pp. 563-573, 586.

7. Movchan, A. A.: On the Stability of a Panel Moving in a Gas. NASA RE 11-21-58W, 1959.

8. Bijlaard, P. P.: Stability of Sandwich Plates. J. Aeron. Sci. (Readers' Forum), vol. 16, no. 9, Sept. 1949, pp. 573-574.

9. Wylie, C. R., Jr.: Advanced Engineering Mathematics. Second ed., McGraw-Hill Book Co., Inc., 1960, p. 34.

TABLE I.- FLUTTER SOLUTIONS FOR PANELS WITH LENGTH-WIDTH RATIOS LESS THAN ONE

a/b	λ'_{cr}	ϕ'_{cr}	α_{cr}	λ'_{cr}	ϕ'_{cr}	α_{cr}	λ'_{cr}	ϕ'_{cr}	α_{cr}	λ'_{cr}	ϕ'_{cr}	α_{cr}	r'
	$k'_x = -4$			$k'_x = -2$			$k'_x = -1$			$k'_x = 0$			
0.0	696.5	25.25	3.495	512.5	17.70	3.024	425.8	14.00	2.774	343.4	10.79	2.477	0.00
.2	704.0	25.51	3.516	519.5	17.95	3.047	432.8	14.55	2.777	349.8	10.99	2.506	
.4	727.9	27.01	3.540	541.1	19.08	3.091	453.3	15.62	2.826	369.3	12.12	2.552	
.6	766.9	29.18	3.600	577.4	20.87	3.176	488.0	16.96	2.944	402.0	13.00	2.708	
.8	822.3	31.36	3.742	629.0	23.32	3.305	537.6	19.34	3.080	449.8	15.88	2.814	
	$k'_x = -4$			$k'_x = -2$			$k'_x = -1$			$k'_x = 0$			
0.0	707.5	28.11	3.168	496.8	18.27	2.859	398.5	13.74	2.668	306.0	9.929	2.407	0.05
.2	715.4	27.74	3.228	503.1	18.52	2.881	404.3	14.47	2.652	311.3	10.13	2.433	
.4	737.0	29.07	3.259	522.0	19.15	2.953	422.1	15.12	2.727	327.6	11.06	2.483	
.6	772.6	30.31	3.368	553.9	21.02	3.021	451.6	16.51	2.826	354.8	12.49	2.581	
.8	823.6	33.54	3.445	598.5	23.38	3.138	493.0	18.48	2.969	393.2	14.48	2.723	
	$k'_x = -4$			$k'_x = -2$			$k'_x = -1$			$k'_x = 0$			
0.0	752.6	32.91	3.094	478.8	19.72	2.816	352.9	13.63	2.643	236.8	8.486	2.383	0.20
.2	759.4	33.58	3.103	483.9	19.85	2.845	357.4	13.96	2.659	240.5	8.682	2.407	
.4	779.1	34.61	3.166	499.4	21.03	2.889	370.7	14.77	2.717	251.5	9.237	2.482	
.6	811.6	36.92	3.247	524.8	22.56	2.986	392.4	16.14	2.813	269.5	10.37	2.585	
.8	855.8	39.96	3.367	559.3	24.77	3.118	422.1	18.00	2.952	294.2	12.08	2.718	
	$k'_x = -4$			$k'_x = -2$			$k'_x = -1$			$k'_x = 0$			
0.0	811.4	40.47	3.445	478.8	22.16	3.104	326.3	14.37	2.860	187.1	7.242	2.549	0.40
.2	817.9	40.59	3.475	483.3	22.65	3.122	330.0	14.49	2.892	189.8	7.610	2.557	
.4	836.7	41.83	3.547	497.0	23.37	3.203	340.8	15.21	2.967	197.7	8.030	2.645	
.6	868.2	44.65	3.658	518.9	25.11	3.316	358.0	16.51	3.083	210.3	8.990	2.763	
.8	909.1	48.62	3.802	548.3	27.48	3.470	381.1	18.37	3.238	227.0	10.20	2.934	
	$k'_x = -4$			$k'_x = -2$			$k'_x = -1$			$k'_x = 0$			
0.0	947.3	57.87	4.814	507.8	28.95	4.319	304.9	16.33	3.916	121.8	5.720	3.221	1.00
.2	953.5	58.22	4.846	511.8	29.38	4.352	307.6	16.58	3.951	123.2	5.856	3.255	
.4	972.8	60.60	4.943	523.5	30.42	4.451	315.6	17.29	4.050	127.4	6.221	3.358	
.6	1003	63.84	5.095	542.1	32.31	4.606	328.3	18.59	4.208	134.0	6.816	3.521	
.8	1042	67.91	5.292	566.3	34.84	4.808	344.8	20.28	4.413	142.6	7.689	3.730	
	$k'_x = -4$			$k'_x = -2$			$k'_x = -1$			$k'_x = 0$			
0.0	1093	79.02	6.154	556.8	37.78	5.644	306.6	19.56	5.183	81.14	4.431	4.135	2.00
.2	1100	79.92	6.191	560.5	38.25	5.682	308.9	19.88	5.222	81.96	4.522	4.176	
.4	1119	82.42	6.299	571.3	39.66	5.791	315.6	20.55	5.334	84.28	4.808	4.292	
.6	1148	86.59	6.465	588.4	41.69	5.964	326.0	21.88	5.510	87.98	5.189	4.479	
.8	1187	91.65	6.682	610.1	44.52	6.183	339.3	23.53	5.734	92.65	5.759	4.714	

TABLE I.- FLUTTER SOLUTIONS FOR PANELS WITH LENGTH-WIDTH RATIOS LESS THAN ONE – Concluded

a/b	λ'_{cr}	ϕ'_{cr}	α_{cr}	λ'_{cr}	ϕ'_{cr}	α_{cr}	λ'_{cr}	ϕ'_{cr}	α_{cr}	λ'_{cr}	ϕ'_{cr}	α_{cr}	r'
		$k'_x = 1$			$k'_x = 2$			$k'_x = 3$			$k'_x = 4$		
0.0	264.9	7.400	2.174	190.9	4.400	1.807	121.8	1.350	1.390	57.98	-1.400	0.8248	0.00
.2	271.0	7.834	2.185	196.7	4.626	1.840	127.2	1.618	1.424	62.88	-1.190	.8785	
.4	289.5	8.554	2.270	214.1	5.338	1.934	143.4	2.348	1.532	77.80	-.5094	1.027	
.6	320.9	9.818	2.406	243.6	6.546	2.088	171.1	3.616	1.703	103.4	+.6876	1.250	
.8	366.1	12.25	2.550	286.4	8.822	2.256	211.2	5.610	1.918	140.7	2.566	1.520	
		$k'_x = 0.9$			$k'_x = 1.859$			$k'_x = 2.7$			$k'_x = 3.6$		
0.0	227.8	6.506	2.144	150.9	3.401	1.760	89.33	0.7496	1.334	30.50	-1.804	0.6333	0.05
.2	232.9	6.859	2.157	155.4	3.585	1.794	93.34	.9243	1.375	33.97	-1.637	.6937	
.4	247.8	7.620	2.224	168.8	4.272	1.876	105.4	1.544	1.481	44.47	-1.107	.8617	
.6	272.8	8.655	2.362	191.5	5.404	2.015	125.8	2.497	1.663	62.33	-.1511	1.106	
.8	308.3	10.80	2.491	223.7	7.057	2.203	155.0	4.149	1.872	87.99	1.330	1.393	
		$k'_x = 0.7$			$k'_x = 1.4$			$k'_x = 1.528$			$k'_x = 2.1$		
0.0	162.5	5.096	2.155	95.58	2.261	1.798	84.27	1.736	1.723	38.05	-0.1841	1.192	0.20
.2	165.7	5.323	2.174	98.15	2.379	1.834	86.76	1.911	1.748	40.01	-.0443	1.229	
.4	175.0	5.812	2.254	105.8	2.877	1.913	94.12	2.330	1.843	45.92	.3000	1.361	
.6	190.4	6.805	2.365	118.5	3.655	2.053	106.3	3.152	1.975	55.69	.9585	1.547	
.8	211.5	8.132	2.527	135.9	4.826	2.232	122.9	4.296	2.159	69.16	1.914	1.786	
		$k'_x = 0.5$			$k'_x = 1.0$			$k'_x = 1.224$			$k'_x = 1.5$		
0.0	124.6	4.416	2.301	68.40	1.829	1.963	45.98	0.8732	1.725	21.62	-0.1593	1.273	0.40
.2	126.7	4.504	2.336	70.02	1.992	1.982	47.34	.9808	1.756	22.67	-.0860	1.322	
.4	133.0	4.972	2.412	74.76	2.324	2.074	51.36	1.281	1.855	25.78	.1730	1.445	
.6	143.2	5.703	2.542	82.41	2.882	2.222	57.87	1.790	2.013	30.81	.5998	1.642	
.8	156.7	6.818	2.706	92.67	3.733	2.407	66.60	2.566	2.207	37.62	1.270	1.871	
		$k'_x = 0.25$			$k'_x = 0.50$			$k'_x = 0.75$			$k'_x = 0.80$		
0.0	81.17	3.526	2.934	44.12	1.637	2.530	12.88	0.1550	1.801	7.824	-0.0650	1.518	1.00
.2	82.27	3.642	2.968	44.88	1.702	2.567	13.28	.2079	1.836	8.143	-.0232	1.565	
.4	85.48	3.905	3.074	47.08	1.908	2.674	14.43	.3378	1.964	9.074	.1042	1.696	
.6	90.53	4.392	3.237	50.54	2.262	2.841	16.25	.5816	2.143	10.54	.3224	1.894	
.8	97.08	5.071	3.448	55.03	2.772	3.054	18.59	.9270	2.373	12.43	.6306	2.146	
		$k'_x = 0.125$			$k'_x = 0.25$			$k'_x = 0.375$			$k'_x = 0.4444$		
0.0	56.42	2.918	3.848	33.28	1.576	3.436	12.68	0.4588	2.724	3.369	0.0000	1.879	2.00
.2	57.05	2.994	3.889	33.71	1.622	3.479	12.90	.4796	2.772	3.476	.0217	1.929	
.4	58.85	3.187	4.010	34.95	1.769	3.602	13.55	.5854	2.892	3.785	.0889	2.068	
.6	61.65	3.518	4.197	36.86	2.007	3.792	14.57	.7337	3.093	4.260	.2030	2.277	
.8	65.21	3.963	4.434	39.29	2.323	4.034	15.84	.9466	3.342	4.860	.3643	2.538	

TABLE II.- FLUTTER SOLUTIONS FOR PANELS WITH LENGTH-WIDTH RATIOS GREATER THAN OR EQUAL TO ONE

a/b	λ_{cr}	ϕ_{cr}	α_{cr}	λ_{cr}	ϕ_{cr}	α_{cr}	λ_{cr}	ϕ_{cr}	α_{cr}	λ_{cr}	ϕ_{cr}	α_{cr}	r
	$k_x = -4$			$k_x = -2$			$k_x = -1$			$k_x = 0$			
1.00	895.4	35.23	3.877	697.0	27.06	3.448	603.0	23.00	3.229	512.5	19.22	2.988	0.0
1.25	644.5	21.59	4.481	471.6	15.58	3.911	391.0	12.85	3.592	314.7	10.18	3.263	
1.50	517.9	15.38	5.117	360.5	10.61	4.405	288.3	8.466	4.009	220.8	6.449	3.586	
1.75	444.6	12.04	5.767	297.6	7.986	4.938	230.7	6.170	4.486	169.5	4.739	3.884	
2.00	398.3	9.906	6.497	258.3	6.475	5.477	195.6	5.016	4.895	138.3	3.726	4.238	
2.50	344.6	7.616	7.965	212.6	4.708	6.747	155.8	3.694	5.847	104.0	2.724	4.958	
3.00	315.7	6.486	9.408	189.7	4.023	7.793	134.9	3.035	6.873	86.38	2.237	5.751	
4.00	286.7	5.375	12.43	166.2	3.259	10.21	114.4	2.434	9.001	69.39	1.801	7.461	
5.00	273.2	4.874	15.50	155.3	2.920	12.67	105.1	2.187	11.08	61.75	1.629	9.118	
7.00	261.1	4.444	21.70	145.6	2.630	17.71	96.75	1.974	15.32	54.98	1.479	12.68	
10.00	254.6	4.218	31.04	140.3	2.479	25.32	92.23	1.859	21.92	51.39	1.406	17.89	
15.00	251.0	4.097	46.69	137.4	2.398	38.09	89.75	1.799	32.93	49.40	1.366	26.81	
20.00	249.7	4.054	62.46	136.4	2.370	50.89	88.87	1.777	44.04	48.68	1.351	35.89	
50.00*	248.2	4.006	157.1	135.2	2.338	128.3	87.84	1.753	111.1	47.85	1.335	90.73	
100.00*	248.1	4.002	314.2	135.1	2.334	256.5	87.73	1.751	222.2	47.77	1.334	181.4	
∞*	248.0	4.000	∞	135.0	2.333	∞	87.70	1.750	∞	47.73	1.333	∞	
	$k_x = -4$			$k_x = -2$			$k_x = -1$			$k_x = 0$			
1.00	888.5	37.42	3.565	656.0	26.70	3.279	546.8	21.74	3.108	442.9	17.14	2.907	0.05
1.25	652.0	22.91	4.121	456.9	15.63	3.723	366.6	12.30	3.486	281.9	9.413	3.174	
1.50	527.0	16.43	4.662	354.4	10.71	4.198	275.3	8.348	3.857	201.9	6.112	3.482	
1.75	453.6	12.45	5.365	294.7	8.109	4.695	222.8	6.211	4.280	156.8	4.457	3.814	
2.00	406.3	10.35	5.976	256.8	6.550	5.221	189.8	4.976	4.717	129.0	3.555	4.140	
2.50	350.7	7.931	7.286	213.0	4.897	6.296	152.2	3.648	5.664	97.86	2.591	4.881	
3.00	320.3	6.677	8.645	189.4	4.047	7.439	132.2	3.001	6.645	81.64	2.143	5.642	
4.00	289.7	5.484	11.40	165.9	3.270	9.713	112.4	2.404	8.685	65.90	1.730	7.309	
5.00	275.2	4.952	14.17	154.9	2.197	12.09	103.3	2.154	10.69	58.51	1.564	8.924	
7.00	262.2	4.486	19.87	145.0	2.619	16.88	95.10	1.933	14.90	52.38	1.420	12.37	
10.00	255.2	4.238	28.43	139.6	2.462	24.13	90.64	1.818	21.27	48.94	1.347	17.60	
15.00	251.3	4.107	42.84	136.7	2.378	36.29	88.19	1.757	32.00	47.05	1.308	26.43	
20.00	249.8	4.059	57.34	135.6	2.349	48.50	87.31	1.736	42.74	46.37	1.294	35.32	
50.00*	248.3	4.007	144.0	134.4	2.315	122.3	86.29	1.712	107.9	45.58	1.279	89.31	
100.00*	248.1	4.002	288.0	134.3	2.312	244.6	86.19	1.709	215.8	45.50	1.277	178.6	
∞*	248.0	4.000	∞	134.2	2.311	∞	86.15	1.709	∞	45.47	1.277	∞	
	$k_x = -4$			$k_x = -2$			$k_x = -1$			$k_x = 0$			
1.00	910.9	43.97	3.516	602.4	27.80	3.275	459.1	20.74	3.106	325.0	14.19	2.899	0.2
1.25	684.3	26.85	3.850	437.6	16.52	3.571	324.1	12.08	3.363	219.2	8.008	3.104	
1.50	557.7	18.58	4.304	347.0	11.32	3.949	250.8	8.146	3.700	162.8	5.335	3.359	
1.75	480.6	14.42	4.743	292.0	8.496	4.385	206.5	5.978	4.118	129.4	3.920	3.675	
2.00	428.1	11.46	5.331	256.2	6.906	4.807	178.3	4.879	4.467	108.1	3.138	3.989	
2.50	367.7	8.722	6.364	213.5	5.104	5.744	144.7	3.569	5.330	83.57	2.308	4.690	
3.00	333.4	7.280	7.420	189.9	4.165	6.778	126.4	2.911	6.262	70.35	1.893	5.484	
4.00	298.0	5.820	9.740	165.9	3.311	8.837	107.9	2.327	8.088	57.37	1.548	6.986	
5.00	281.0	5.166	12.08	154.4	2.931	10.93	99.11	2.061	10.04	51.28	1.393	8.601	
7.00	265.5	4.598	16.86	144.0	2.603	15.19	91.22	1.840	13.86	45.56	1.253	12.16	
10.00	256.9	4.296	24.12	138.3	2.428	21.76	86.88	1.721	19.87	42.88	1.198	16.94	
15.00	252.1	4.132	36.35	135.1	2.333	32.84	84.46	1.658	29.89	41.24	1.163	25.44	
20.00	250.2	4.070	48.72	133.9	2.301	43.87	83.59	1.636	39.92	40.64	1.151	34.00	
50.00*	248.3	4.009	122.2	132.6	2.263	110.4	82.57	1.611	100.9	39.95	1.136	86.02	
100.00*	248.1	4.002	244.4	132.5	2.259	220.7	82.46	1.608	201.7	39.87	1.135	172.0	
∞*	248.0	4.000	∞	132.4	2.258	∞	82.43	1.607	∞	39.85	1.134	∞	

*Denotes preflutter solution for this value of a/b.

TABLE II.- FLUTTER SOLUTIONS FOR PANELS WITH LENGTH-WIDTH RATIOS GREATER THAN OR EQUAL TO ONE – Continued

a/b	λ_{cr}	ϕ_{cr}	α_{cr}	λ_{cr}	ϕ_{cr}	α_{cr}	λ_{cr}	ϕ_{cr}	α_{cr}	λ_{cr}	ϕ_{cr}	α_{cr}	r
		$k_x = -4$			$k_x = -2$			$k_x = -1$			$k_x = 0$		
1.00	960.0	52.41	3.999	583.9	30.52	3.659	409.2	20.69	3.431	247.5	12.03	3.122	0.4
1.25	729.1	31.89	4.075	433.6	18.13	3.751	297.6	12.12	3.526	172.9	6.939	3.194	
1.50	596.0	21.89	4.330	348.1	12.38	3.991	234.6	8.182	3.759	131.6	4.646	3.386	
1.75	512.6	16.57	4.667	294.9	9.253	4.318	195.8	6.106	4.057	106.4	3.453	3.639	
2.00	456.7	13.41	5.042	259.4	7.437	4.667	170.0	4.863	4.405	89.97	2.754	3.939	
2.50	388.1	9.828	5.912	216.4	5.402	5.489	139.1	3.528	5.181	70.49	2.012	4.628	
3.00	349.0	7.999	6.842	192.2	4.374	6.372	121.9	2.888	5.961	59.89	1.673	5.315	
4.00	308.0	6.238	8.816	167.0	3.415	8.190	104.1	2.260	7.718	49.12	1.354	6.838	
5.00	288.0	5.434	10.89	154.8	2.978	10.12	95.58	1.989	9.492	44.06	1.223	8.327	
7.00	269.5	4.744	15.10	143.6	2.603	14.06	87.80	1.754	13.16	39.47	1.107	11.50	
10.00	259.0	4.370	21.50	137.3	2.405	20.04	83.44	1.631	18.74	36.92	1.048	16.33	
15.00	253.1	4.168	32.28	133.8	2.297	30.10	80.99	1.564	28.15	35.50	1.016	24.58	
20.00	250.8	4.088	43.41	132.4	2.257	40.51	80.11	1.541	37.62	34.98	1.004	32.84	
50.00*	248.4	4.011	108.8	131.0	2.216	101.5	79.06	1.513	95.05	34.37	.9915	83.09	
100.00*	248.1	4.002	217.5	130.8	2.211	203.0	78.97	1.511	190.1	34.32	.9902	166.1	
∞*	248.0	4.000	∞	130.8	2.210	∞	78.92	1.509	∞	34.29	.9897	∞	
		$k_x = -4$			$k_x = -2$			$k_x = -1$			$k_x = 0$		
1.00	1 089	73.71	5.528	594.8	38.09	5.047	364.1	22.31	4.656	152.6	8.771	3.978	1.0
1.25	835.5	44.32	5.326	451.4	22.74	4.834	273.1	13.25	4.442	111.1	5.161	3.788	
1.50	684.6	30.22	5.281	366.7	15.38	4.796	219.8	8.920	4.419	87.02	3.469	3.801	
1.75	586.3	22.57	5.343	312.2	11.39	4.884	185.6	6.582	4.526	71.86	2.589	3.932	
2.00	519.7	17.72	5.512	275.0	8.950	5.066	162.4	5.215	4.711	61.70	2.100	4.102	
2.50	435.3	12.51	6.015	228.6	6.333	5.594	133.7	3.674	5.272	49.33	1.537	4.637	
3.00	385.9	9.841	6.667	201.6	4.993	6.261	117.2	2.923	5.932	42.32	1.268	5.241	
4.00	332.5	7.293	8.195	172.8	3.736	7.763	99.53	2.207	7.443	35.02	1.018	6.591	
5.00	305.5	6.134	9.867	158.4	3.165	9.404	90.97	1.910	8.938	31.46	.9106	7.996	
7.00	279.8	5.123	13.39	144.8	2.672	12.81	82.85	1.636	12.23	27.46	.7955	11.29	
10.00	264.7	4.570	18.85	136.9	2.405	18.08	78.17	1.490	17.31	26.34	.7698	15.59	
15.00	255.9	4.263	28.10	132.3	2.258	27.04	75.48	1.409	25.98	25.28	.7439	23.35	
20.00	252.6	4.151	37.45	130.6	2.205	36.05	74.49	1.381	34.60	24.90	.7344	31.17	
50.00*	248.7	4.019	94.31	128.6	2.143	90.78	73.30	1.347	87.27	24.44	.7240	83.56	
100.00*	248.2	4.005	188.5	128.3	2.136	181.5	73.17	1.344	174.5	24.39	.7228	167.1	
∞*	248.0	4.000	∞	128.3	2.134	∞	73.16	1.343	∞	24.35	.7223	∞	
		$k_x = -4$			$k_x = -2$			$k_x = -1$			$k_x = 0$		
1.00	1 231	98.00	6.933	635.3	47.94	6.439	354.7	25.55	5.994	97.89	6.396	4.978	2.0
1.25	951.0	59.19	6.694	487.6	28.71	6.181	270.3	15.25	5.718	72.87	3.799	4.670	
1.50	780.4	40.10	6.595	398.3	19.41	6.066	219.6	10.26	5.591	58.14	2.617	4.539	
1.75	667.9	29.52	6.591	339.7	14.27	6.051	186.6	7.537	5.568	48.59	1.949	4.533	
2.00	589.3	23.04	6.657	299.0	11.14	6.108	163.7	5.896	5.626	41.99	1.542	4.624	
2.50	488.6	15.89	6.935	247.2	7.675	6.388	134.7	4.096	5.921	33.98	1.142	4.976	
3.00	428.3	12.20	7.357	216.4	5.936	6.824	117.7	3.180	6.385	29.28	.9353	5.461	
4.00	361.7	8.664	8.488	182.6	4.250	8.005	99.12	2.318	7.593	24.30	.7395	6.682	
5.00	327.0	7.051	9.853	165.3	3.494	9.388	89.65	1.931	8.984	21.81	.6542	8.019	
7.00	293.1	5.631	12.91	148.5	2.831	12.44	80.57	1.595	11.97	19.48	.5818	10.85	
10.00	272.5	4.847	17.82	138.3	2.468	17.29	75.18	1.411	16.75	18.12	.5434	15.26	
15.00	260.0	4.401	26.28	132.3	2.264	25.60	71.99	1.309	24.86	17.34	.5223	22.76	
20.00	255.1	4.235	34.87	129.9	2.187	34.10	70.78	1.272	33.08	17.05	.5148	30.32	
50.00*	249.0	4.032	87.35	127.1	2.097	85.34	69.29	1.227	83.18	16.69	.5059	76.54	
100.00*	248.3	4.008	174.6	126.8	2.087	170.6	69.11	1.222	166.3	16.65	.5050	153.0	
∞*	248.0	4.000	∞	126.7	2.085	∞	69.05	1.221	∞	16.65	.5047	∞	

*Denotes preflutter solution for this value of a/b.

TABLE II.- FLUTTER SOLUTIONS FOR PANELS WITH LENGTH-WIDTH RATIOS GREATER THAN OR EQUAL TO ONE – Continued

a/b	λ_{cr}	ϕ_{cr}	α_{cr}	λ_{cr}	ϕ_{cr}	α_{cr}	λ_{cr}	ϕ_{cr}	α_{cr}	λ_{cr}	ϕ_{cr}	α_{cr}	r
		$k_x = 1$			$k_x = 2$			$k_x = 3$			$k_x = 4$		
1.00	426.0	15.37	2.747	343.4	11.79	2.477	264.6	8.200	2.190	190.9	5.287	1.818	0.0
1.25	242.8	7.692	2.897	175.8	5.419	2.477	114.0	3.325	1.981	58.13	1.425	1.324	
1.50	158.5	4.757	3.059	101.7	3.131	2.477	51.31	1.690	1.724	8.359	.4618	.4498	
1.75	113.6	3.367	3.246	64.07	2.151	2.477	21.95	1.121	1.364	**			
2.00	87.14	2.620	3.456	42.92	1.674	2.477	7.247	.9106	.8275				
2.50	58.80	1.877	3.976	21.97	1.276	2.477	**						
3.00	45.07	1.600	4.405	12.72	1.133	2.477							
4.00	32.29	1.342	5.477	5.365	1.042	2.477							
5.00	26.66	1.243	6.539	2.747	1.017	2.477							
7.00	21.93	1.160	9.002	1.001	1.005	2.477							
10.00	19.41	1.120	12.70	.3434	1.001	2.477							
15.00	18.03	1.099	18.97	.1017	1.000	2.477							
20.00	17.54	1.092	25.32	.0429	1.000	2.477							
50.00*	16.96	1.084	64.18	.0027	1.000	2.565							
100.00*	16.90	1.084	128.3	.0003	1.000	2.565							
∞*	16.88	1.083	∞	.0000	1.000	2.565							
		$k_x = 0.9$			$k_x = 1.859$			$k_x = 2.7$			$k_x = 3.6$		
1.00	354.2	13.21	2.698	265.6	9.506	2.414	193.2	6.514	2.108	122.0	3.444	1.705	0.05
1.25	210.8	6.926	2.859	141.2	4.588	2.424	86.11	2.727	1.930	34.36	.9302	1.159	
1.50	141.3	4.328	3.058	83.48	2.726	2.439	39.39	1.483	1.683	.8032	.3605	.06165	
1.75	103.2	3.145	3.242	53.27	1.919	2.448	16.90	1.035	1.330	**			
2.00	80.30	2.463	3.475	36.00	1.520	2.458	5.447	.8706	.7860				
2.50	55.41	1.819	3.953	18.63	1.189	2.458	**						
3.00	42.93	1.530	4.473	10.84	1.067	2.459							
4.00	31.27	1.288	5.590	4.599	.9883	2.479							
5.00	26.12	1.192	6.749	2.361	.9672	2.479							
7.00	21.69	1.113	9.242	.8626	.9563	2.479							
10.00	19.33	1.076	13.00	.2962	.9533	2.480							
15.00	18.04	1.056	19.44	.0878	.9525	2.480							
20.00	17.57	1.049	25.96	.0371	.9525	2.481							
50.00*	17.03	1.041	65.78	.0023	.9524	2.565							
100.00*	16.98	1.040	131.5	.0003	.9524	2.565							
∞*	16.96	1.040	∞	.0000	.9524	2.565							
		$k_x = 0.7$			$k_x = 1.4$			$k_x = 1.528$			$k_x = 2.1$		
1.00	237.8	10.20	2.692	157.6	6.537	2.427	143.9	5.883	2.374	86.24	3.376	2.024	0.2
1.25	152.1	5.542	2.840	91.48	3.371	2.468	81.26	3.003	2.384	39.50	1.578	1.831	
1.50	107.2	3.637	3.017	58.08	2.177	2.507	49.97	1.940	2.382	17.69	1.010	1.540	
1.75	81.21	2.673	3.233	39.48	1.606	2.578	32.74	1.445	2.399	6.807	.8136	1.092	
2.00	64.97	2.139	3.467	28.32	1.318	2.647	22.53	1.198	2.412	1.209	.7419	.3593	
2.50	46.66	1.597	4.004	16.47	1.060	2.800	11.93	.9876	2.422	**			
3.00	37.15	1.358	4.547	10.81	.9635	2.921	7.034	.9079	2.443				
4.00	27.99	1.150	5.704	5.906	.8879	3.305	3.025	.8574	2.456				
5.00	23.83	1.063	6.959	3.940	.8634	3.718	1.563	.8432	2.461				
7.00	20.21	.9938	9.536	2.419	.8476	4.636	.5743	.8359	2.479				
10.00	18.24	.9586	13.53	1.668	.8411	5.883	.1978	.8340	2.479				
15.00	17.16	.9404	20.28	1.314	.8377	8.879	.05875	.8334	2.479				
20.00	16.77	.9344	27.07	1.183	.8369	11.72	.02480	.8333	2.479				
50.00*	16.31	.9270	68.48	1.032	.8358	29.66	.0016	.8333	2.565				
100.00*	16.26	.9263	136.9	1.014	.8357	59.16	.0002	.8333	2.565				
∞*	16.24	.9260	∞	1.009	.8357	∞	.0000	.8333	2.565				

*Denotes preflutter solution for this value of a/b.

**$\bar{A} > 5$, see appendix C.

TABLE II.- FLUTTER SOLUTIONS FOR PANELS WITH LENGTH-WIDTH RATIOS GREATER THAN OR EQUAL TO ONE – Concluded

a/b	λ_{cr}	ϕ_{cr}	α_{cr}	λ_{cr}	ϕ_{cr}	α_{cr}	λ_{cr}	ϕ_{cr}	α_{cr}	λ_{cr}	ϕ_{cr}	α_{cr}	r
		$k_x = 0.5$			$k_x = 1.0$			$k_x = 1.224$			$k_x = 1.5$		
1.00	173.2	8.178	2.917	105.2	4.904	2.620	77.25	3.602	2.437	45.95	2.172	2.132	0.4
1.25	116.5	4.661	2.967	65.69	2.725	2.621	45.29	1.989	2.384	23.02	1.219	1.928	
1.50	85.50	3.127	3.112	44.65	1.844	2.684	28.60	1.373	2.361	11.63	.8744	1.717	
1.75	66.87	2.320	3.336	32.36	1.418	2.781	19.11	1.083	2.368	5.578	.7507	1.412	
2.00	54.89	1.883	3.564	24.68	1.186	2.901	13.34	.9362	2.379	2.240	.6975	.9850	
2.50	40.49	1.382	4.212	16.11	.9615	3.205	7.201	.8072	2.413	**			
3.00	33.48	1.216	4.674	11.76	.8690	3.511	4.297	.7602	2.424				
4.00	26.08	1.027	5.922	7.706	.7938	4.212	1.871	.7289	2.458				
5.00	22.64	.9475	7.227	5.943	.7650	4.999	.9731	.7205	2.458				
7.00	19.59	.8830	9.928	4.464	.7439	6.623	.3595	.7160	2.459				
10.00	17.91	.8500	14.09	3.688	.7341	9.191	.1242	.7147	2.479				
15.00	16.98	.8326	21.12	3.267	.7291	13.67	.0370	.7144	2.479				
20.00	16.64	.8262	28.29	3.116	.7275	18.19	.0156	.7143	2.480				
50.00*	16.24	.8197	71.48	2.937	.7255	46.22	.0010	.7143	2.565				
100.00*	16.20	.8190	142.9	2.918	.7253	92.34	.0001	.7143	2.565				
∞*	16.19	.8187	∞	2.912	.7253	∞	.0000	.7143	2.565				
		$k_x = 0.25$			$k_x = 0.50$			$k_x = 0.75$			$k_x = 0.80$		
1.00	104.8	5.948	3.697	60.29	3.417	3.307	21.27	1.342	2.657	14.66	1.046	2.423	1.0
1.25	74.85	3.500	3.520	41.53	2.040	3.149	13.04	.8954	2.466	8.330	.7238	2.200	
1.50	57.65	2.390	3.535	30.89	1.434	3.162	8.507	.7044	2.399	4.947	.5999	2.055	
1.75	46.89	1.799	3.671	24.32	1.125	3.268	5.830	.6172	2.368	3.004	.5465	1.918	
2.00	39.73	1.467	3.856	20.00	.9488	3.427	4.153	.5709	2.371	1.831	.5217	1.756	
2.50	31.07	1.117	4.335	14.88	.7690	3.843	2.305	.5307	2.379	.6277	.5020	1.338	
3.00	26.23	.9464	4.903	12.07	.6862	4.308	1.400	.5151	2.410	.1194	.4970	.5663	
4.00	21.24	.7910	6.171	9.247	.6129	5.366	.6225	.5051	2.424	**			
5.00	18.83	.7258	7.465	7.918	.5822	6.503	.3270	.5021	2.449				
7.00	16.64	.6697	10.28	6.729	.5577	8.887	.1220	.5006	2.456				
10.00	15.41	.6408	14.57	6.069	.5451	12.56	.0424	.5001	2.466				
15.00	14.71	.6254	21.82	5.700	.5385	18.76	.0126	.5000	2.479				
20.00	14.45	.6199	29.16	5.565	.5362	25.00	.0053	.5000	2.479				
50.00*	14.15	.6136	73.74	5.405	.5336	63.48	.0003	.5000	2.565				
100.00*	14.11	.6129	147.4	5.389	.5333	126.9	.00004	.5000	2.565				
∞*	14.10	.6127	∞	5.383	.5332	∞	.00000	.5000	2.565				
		$k_x = 0.125$			$k_x = 0.25$			$k_x = 0.375$			$k_x = 0.4444$		
1.00	69.31	4.517	4.709	42.09	2.742	4.312	17.30	1.219	3.628	5.545	0.5716	2.836	2.0
1.25	51.11	2.695	4.395	30.35	1.690	3.970	12.01	.8024	3.336	3.460	.4428	2.569	
1.50	40.39	1.857	4.265	23.77	1.178	3.884	8.964	.6157	3.249	2.297	.3901	2.456	
1.75	33.53	1.408	4.266	19.45	.9231	3.891	6.996	.5104	3.313	1.597	.3661	2.399	
2.00	28.86	1.142	4.361	16.57	.7675	4.010	5.796	.4672	3.374	1.151	.3536	2.374	
2.50	23.09	.8584	4.729	13.01	.6093	4.374	4.280	.4122	3.697	.6503	.3420	2.384	
3.00	19.77	.7174	5.239	10.98	.5319	4.859	3.441	.3869	4.094	.4000	.3378	2.389	
4.00	16.26	.5902	6.414	8.871	.4617	5.993	2.592	.3651	5.006	.1803	.3348	2.407	
5.00	14.52	.5347	7.705	7.836	.4320	7.207	2.190	.3560	6.024	.0955	.3339	2.435	
7.00	12.91	.4873	10.47	6.882	.4069	9.812	1.829	.3488	8.107	.0359	.3335	2.445	
10.00	11.97	.4623	14.74	6.337	.3938	13.84	1.628	.3451	11.45	.0125	.3334	2.471	
15.00	11.44	.4488	22.00	6.026	.3868	20.68	1.515	.3431	17.14	.0038	.3334	2.477	
20.00	11.24	.4439	29.36	5.911	.3843	27.60	1.474	.3425	22.87	.0016	.3333	2.485	
50.00*	11.00	.4384	74.09	5.775	.3814	69.78	1.424	.3417	58.02	.0001	.3333	2.565	
100.00*	10.97	.4377	148.1	5.759	.3811	139.5	1.420	.3416	116.0	.00001	.3333	2.565	
∞*	10.96	.4375	∞	5.753	.3810	∞	1.418	.3416	∞	.00000	.3333	2.565	

*Denotes preflutter solution for this value of a/b.

**$\overline{A} > 5$, see appendix C.

TABLE III.- COMPARISON OF PREFLUTTER AND EXACT FLUTTER SOLUTIONS FOR $\frac{a}{b} = 20$

r	k_x	λ_{cr}	λ_p
0	-4	249.7	249.3
	-2	136.4	136.0
	-1	88.87	88.58
	0	48.68	48.45
	1	17.54	17.39
	2	.0429	.0422
0.05	-4	249.8	249.4
	-2	135.6	135.3
	-1	87.31	87.02
	0	46.37	46.15
	.9	17.57	17.43
	1.859	.0371	.0364
0.2	-4	250.2	249.8
	-2	133.9	133.6
	-1	83.59	83.31
	0	40.64	40.46
	.7	16.77	16.65
	1.4	1.183	1.153
	1.528	.0248	.0244
0.4	-4	250.8	250.3
	-2	132.4	132.1
	-1	80.11	79.84
	0	34.98	34.82
	.5	16.64	16.54
	1.0	3.116	3.073
	1.224	.0156	.0156
1	-4	252.6	251.8
	-2	130.6	130.2
	-1	74.49	74.25
	0	24.90	24.78
	.25	14.45	14.38
	.5	5.565	5.525
	.75	.0053	.0053
2	-4	255.1	254.3
	-2	129.9	129.5
	-1	70.78	70.51
	0	17.05	16.97
	.125	11.24	11.18
	.250	5.911	5.880
	.375	1.474	1.462
	.4444	.0016	.0016

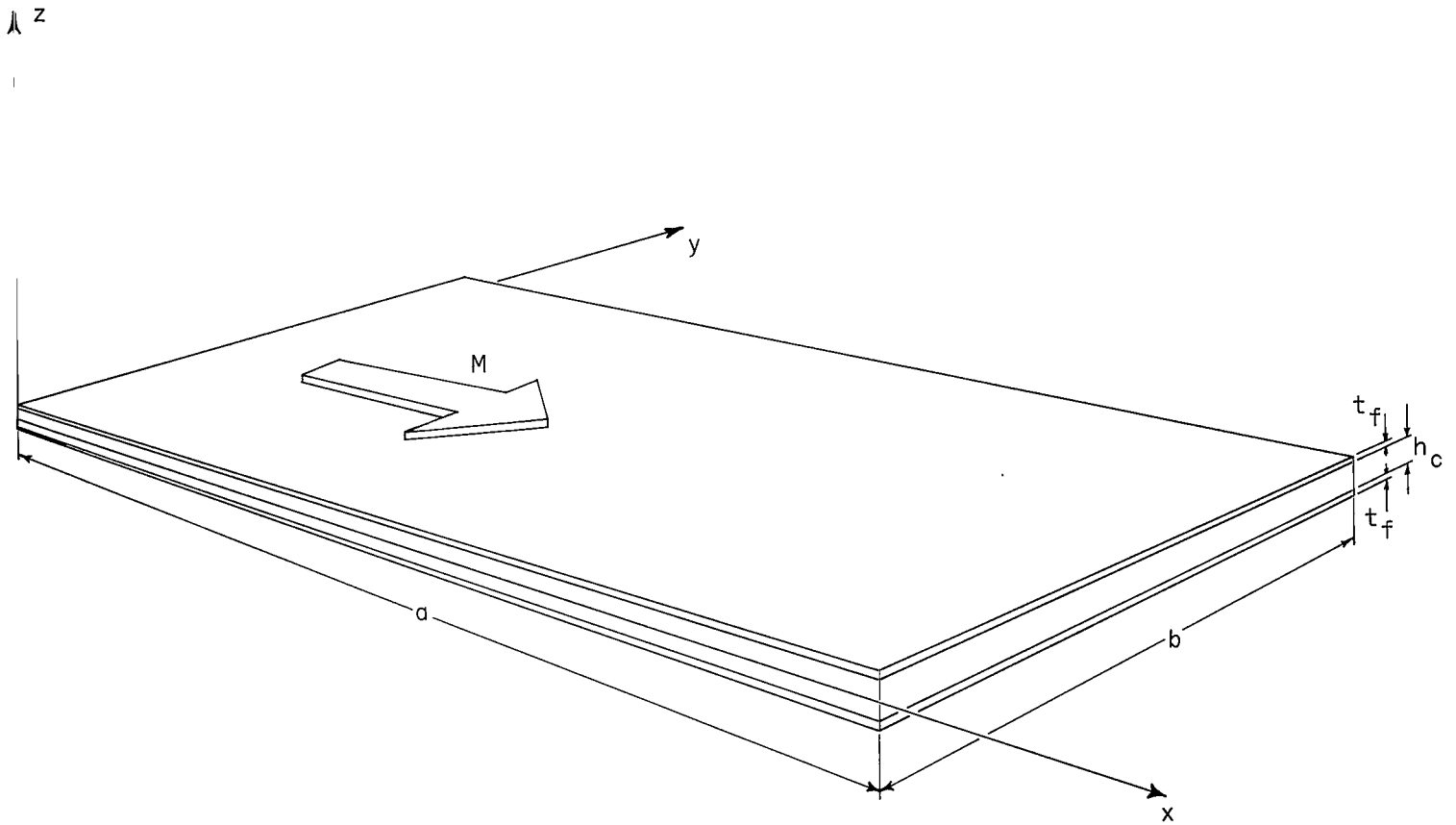

Figure 1.- Panel geometry, coordinate system, and flow direction.

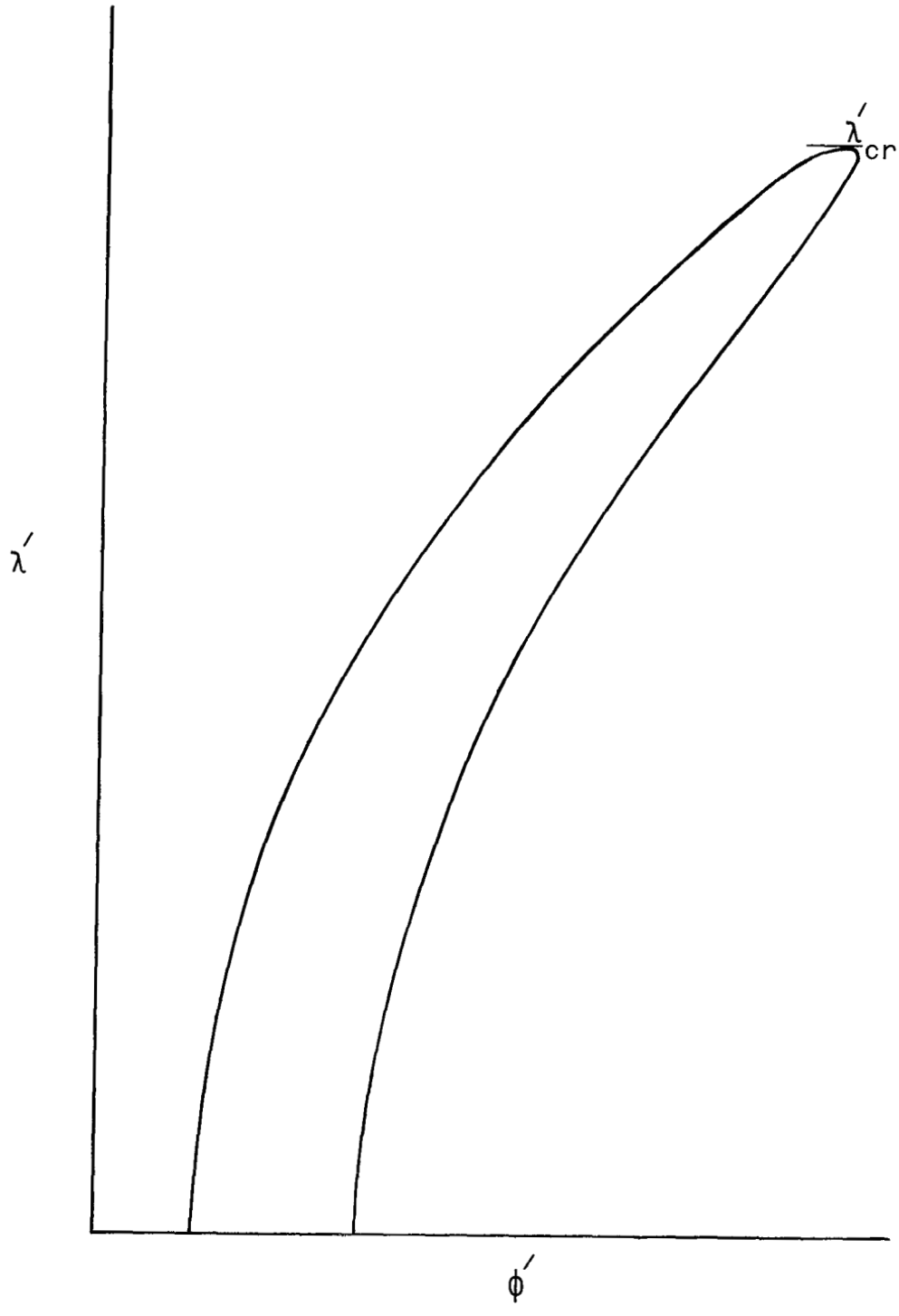

Figure 2.- Frequency loop illustrating λ'_{cr}.

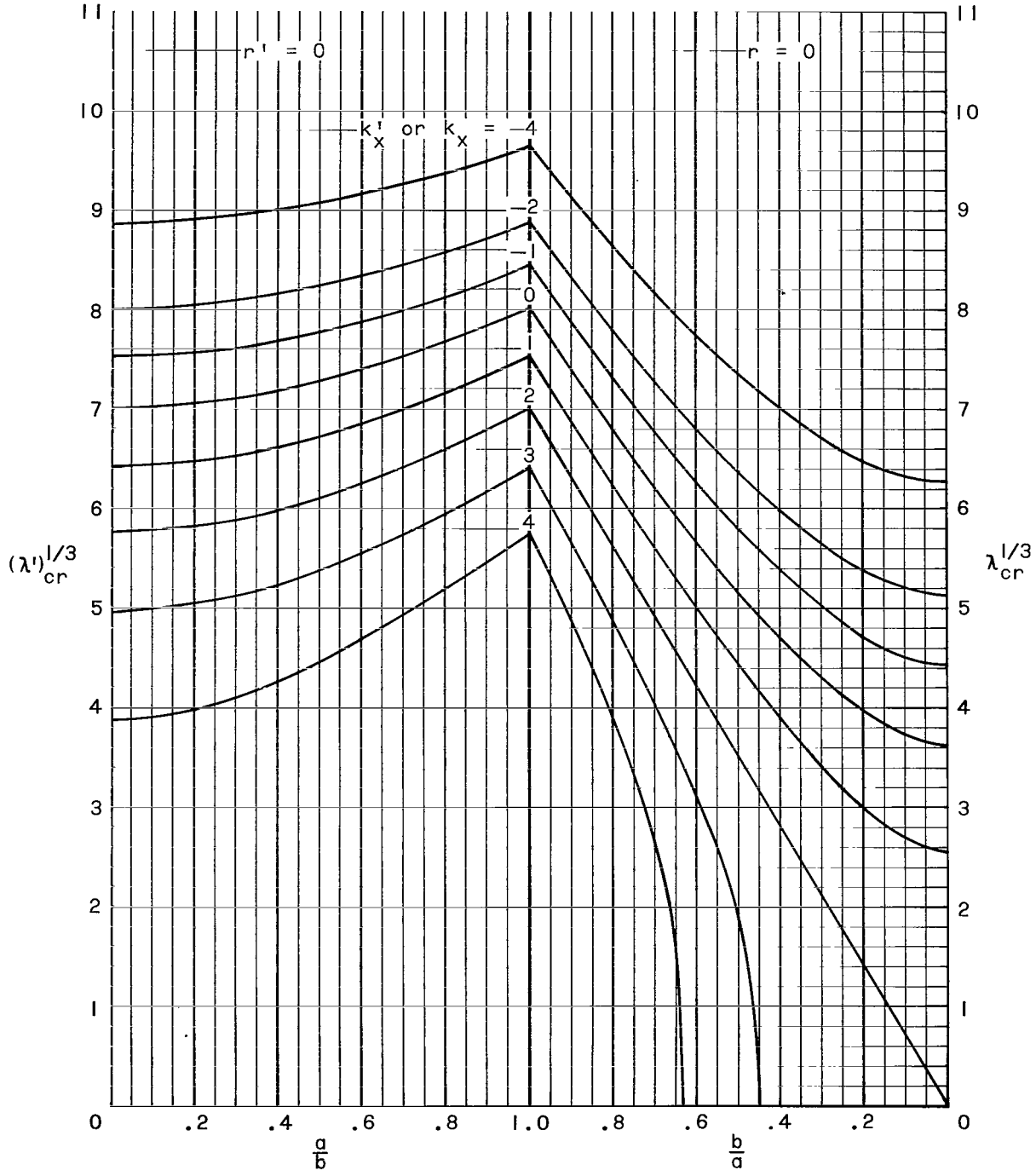

(a) r or r' = 0.

Figure 3.- Flutter values of dynamic pressure parameter.

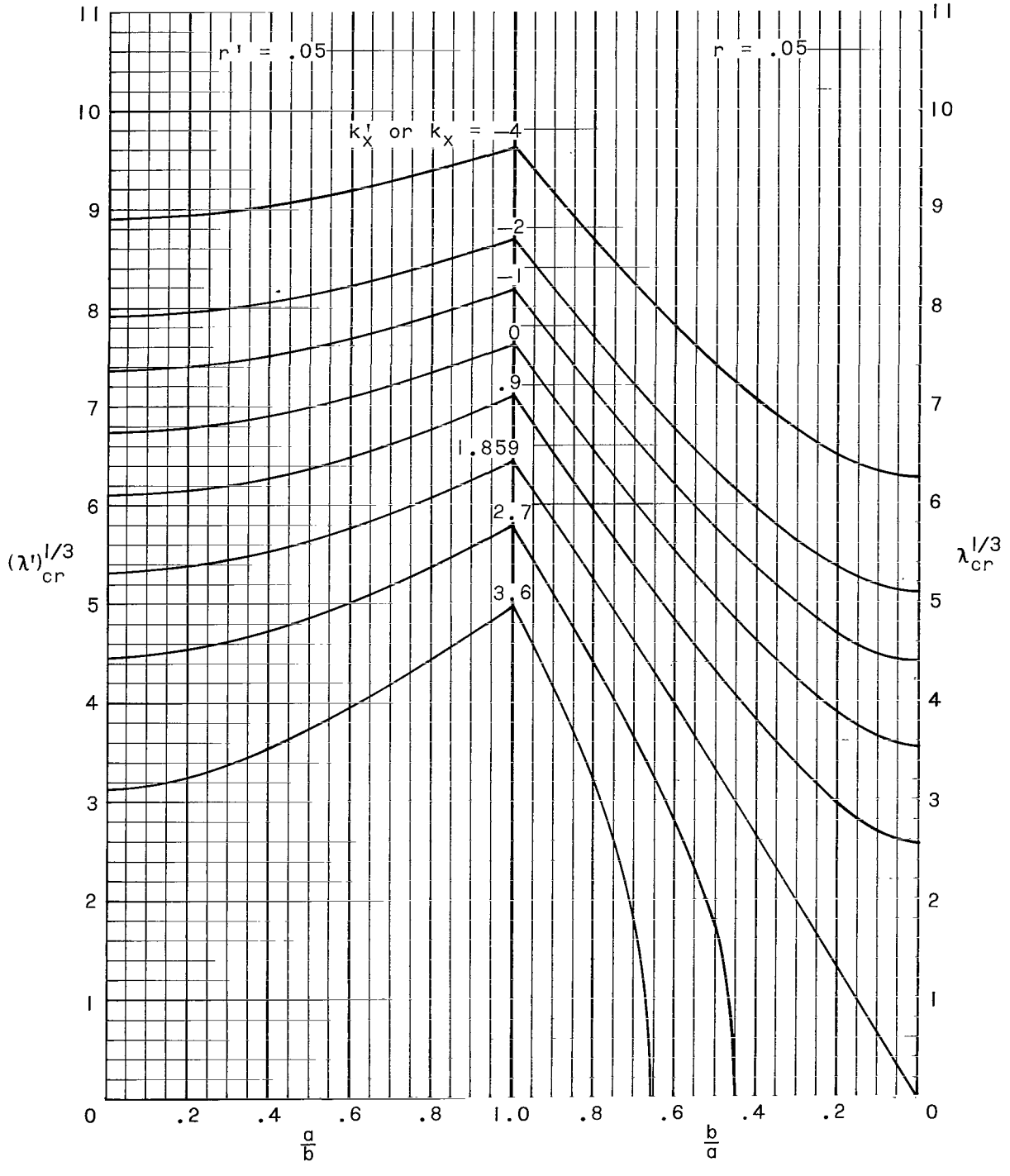

(b) r or r' = 0.05.

Figure 3.- Continued.

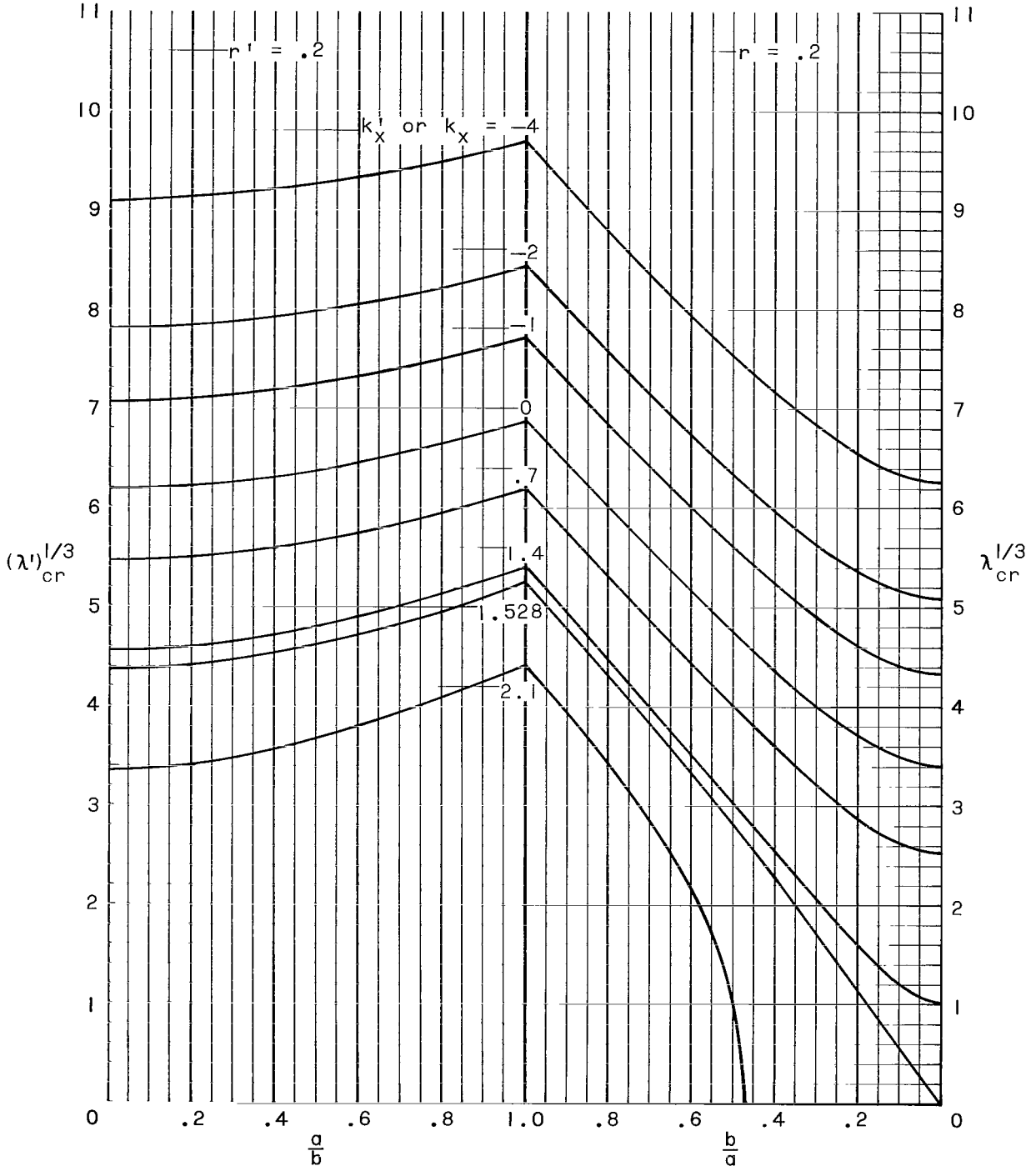

(c) r or r' = 0.2.

Figure 3.- Continued.

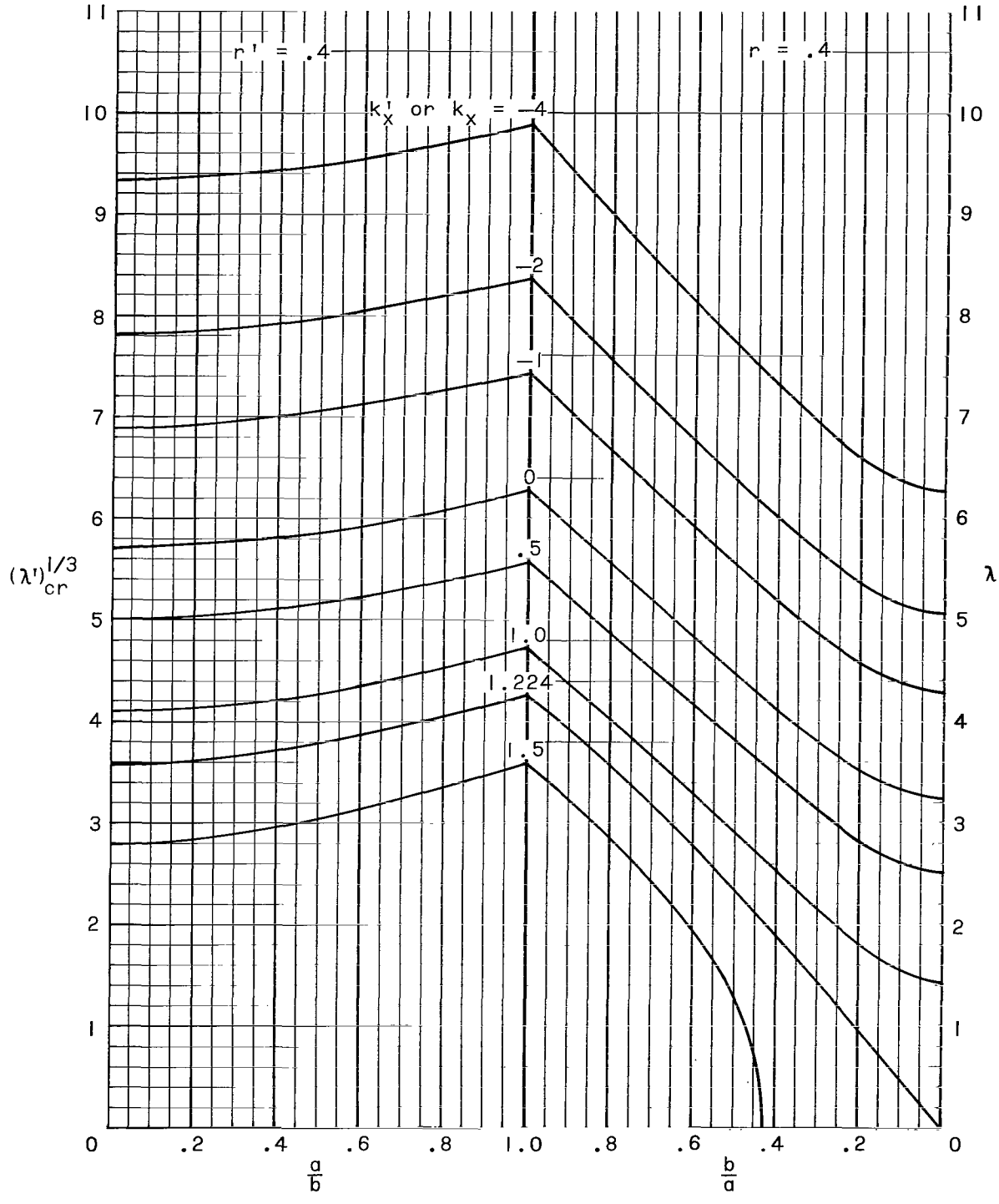

(d) r or r' = 0.4.

Figure 3.- Continued.

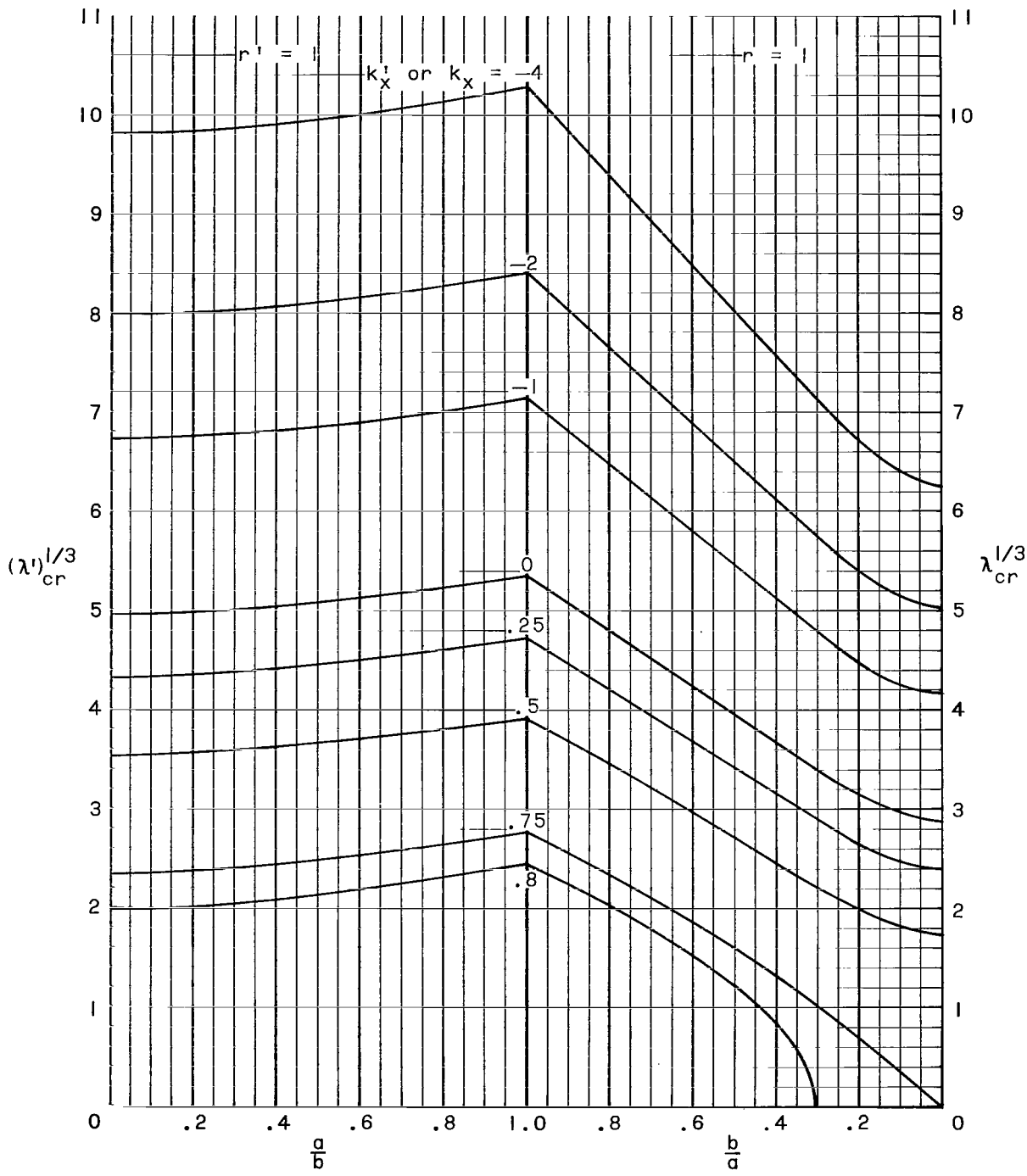

(e) r or r' = 1.0.

Figure 3.- Continued.

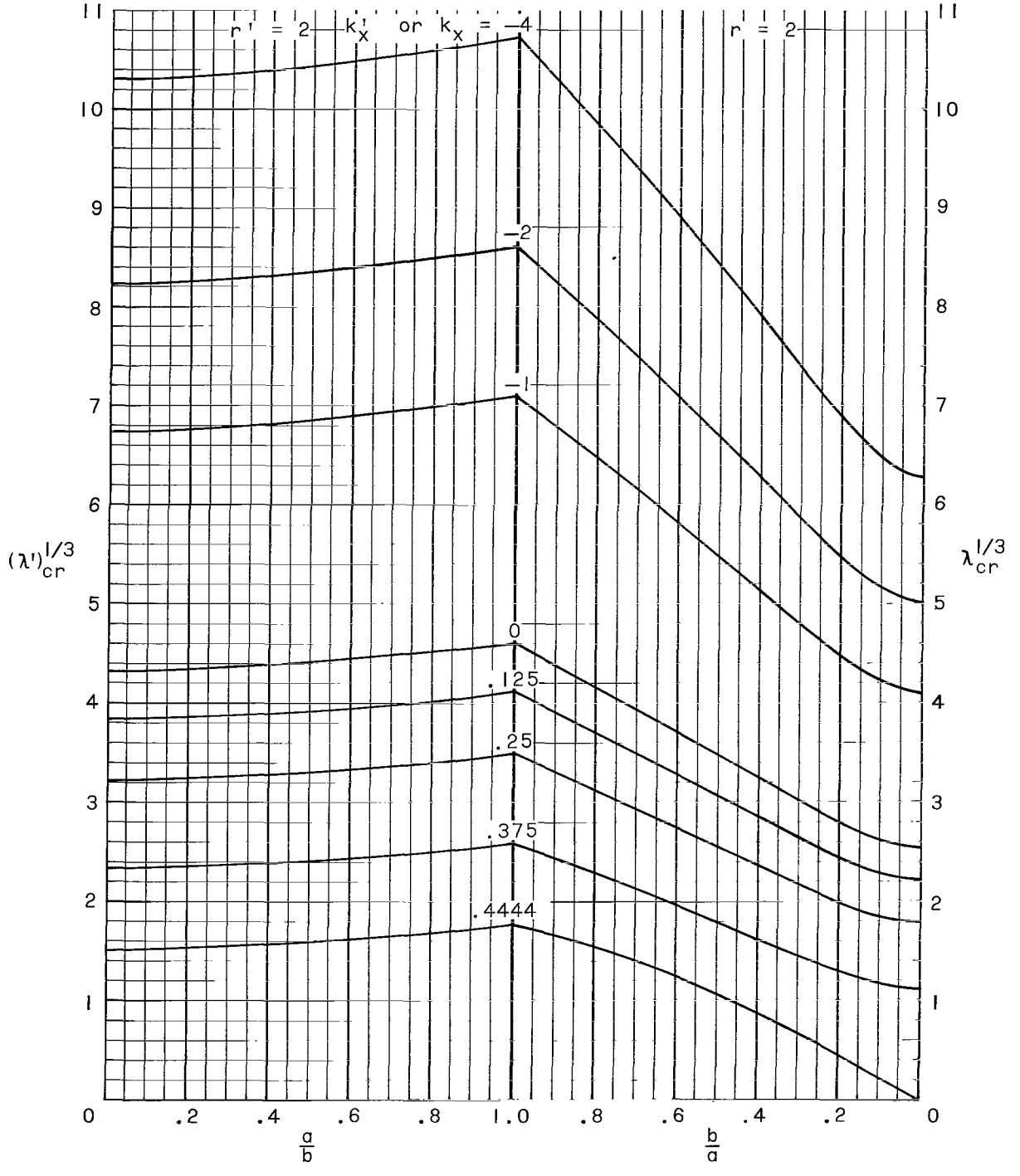

(f) r or r' = 2.0.

Figure 3.- Concluded.

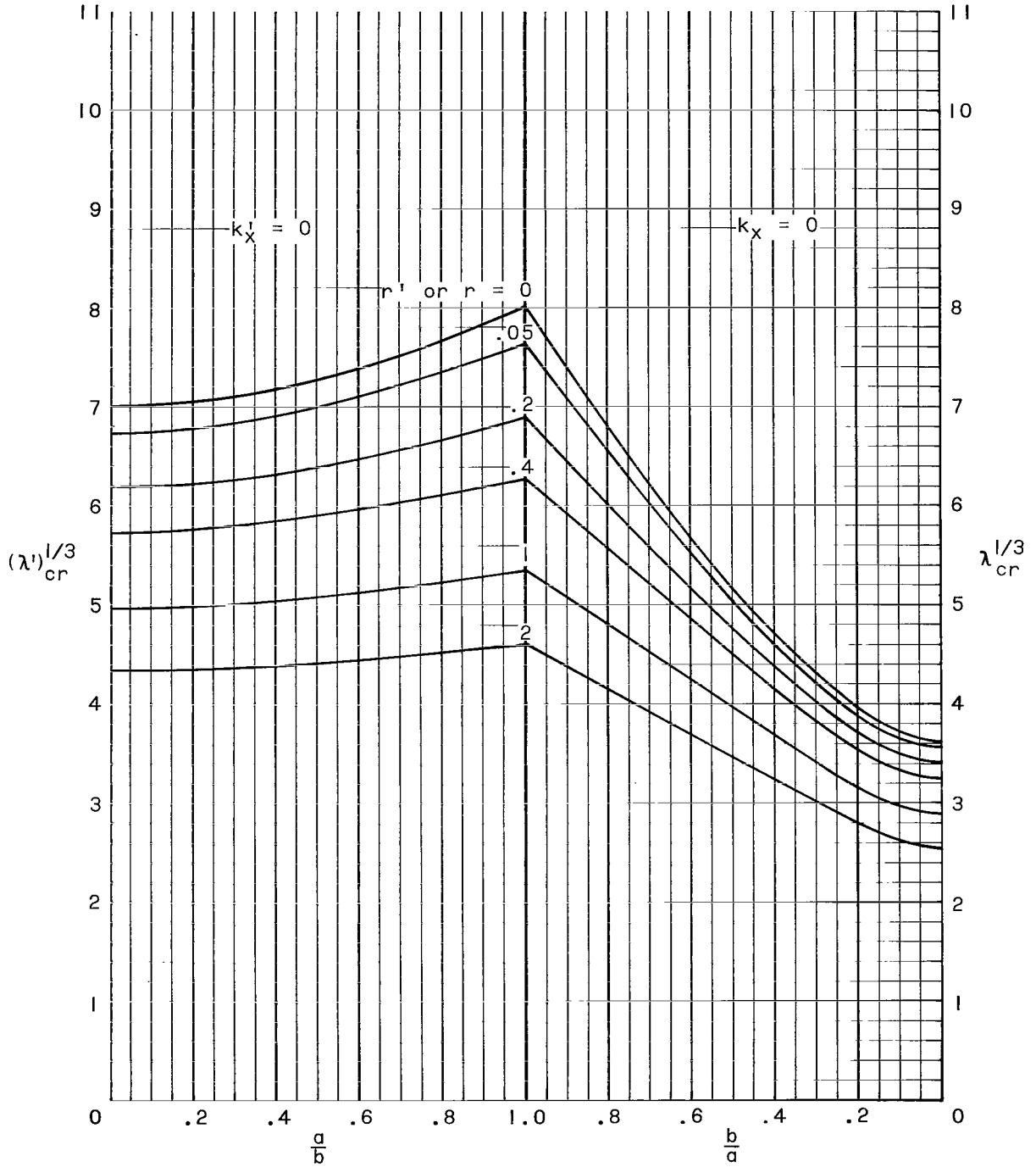

Figure 4.- Flutter values of dynamic-pressure parameter. k_x or k'_x = 0.0.

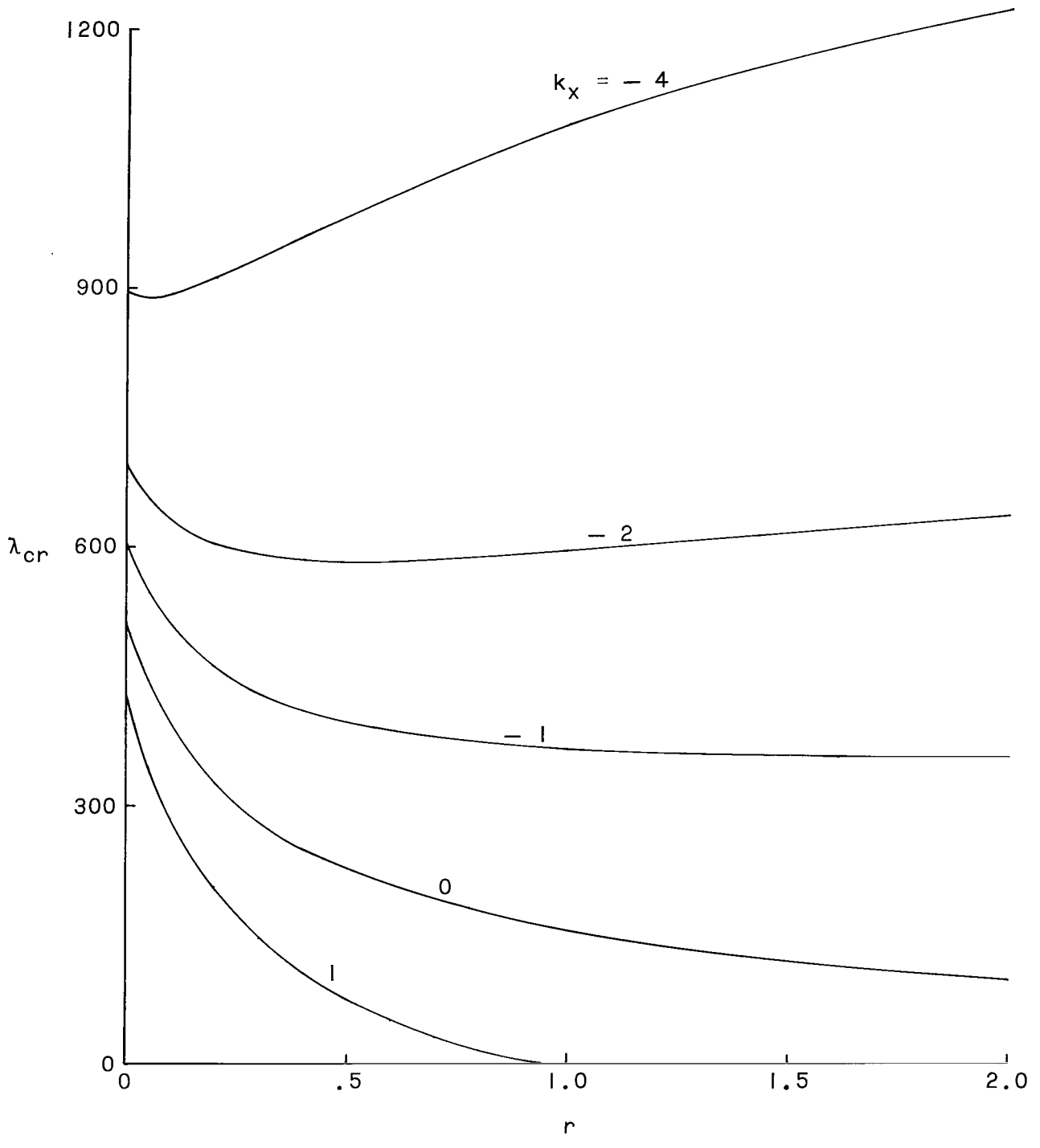

Figure 5.- Effect of transverse shear flexibility and stress on λ_{cr}. a/b = 1.

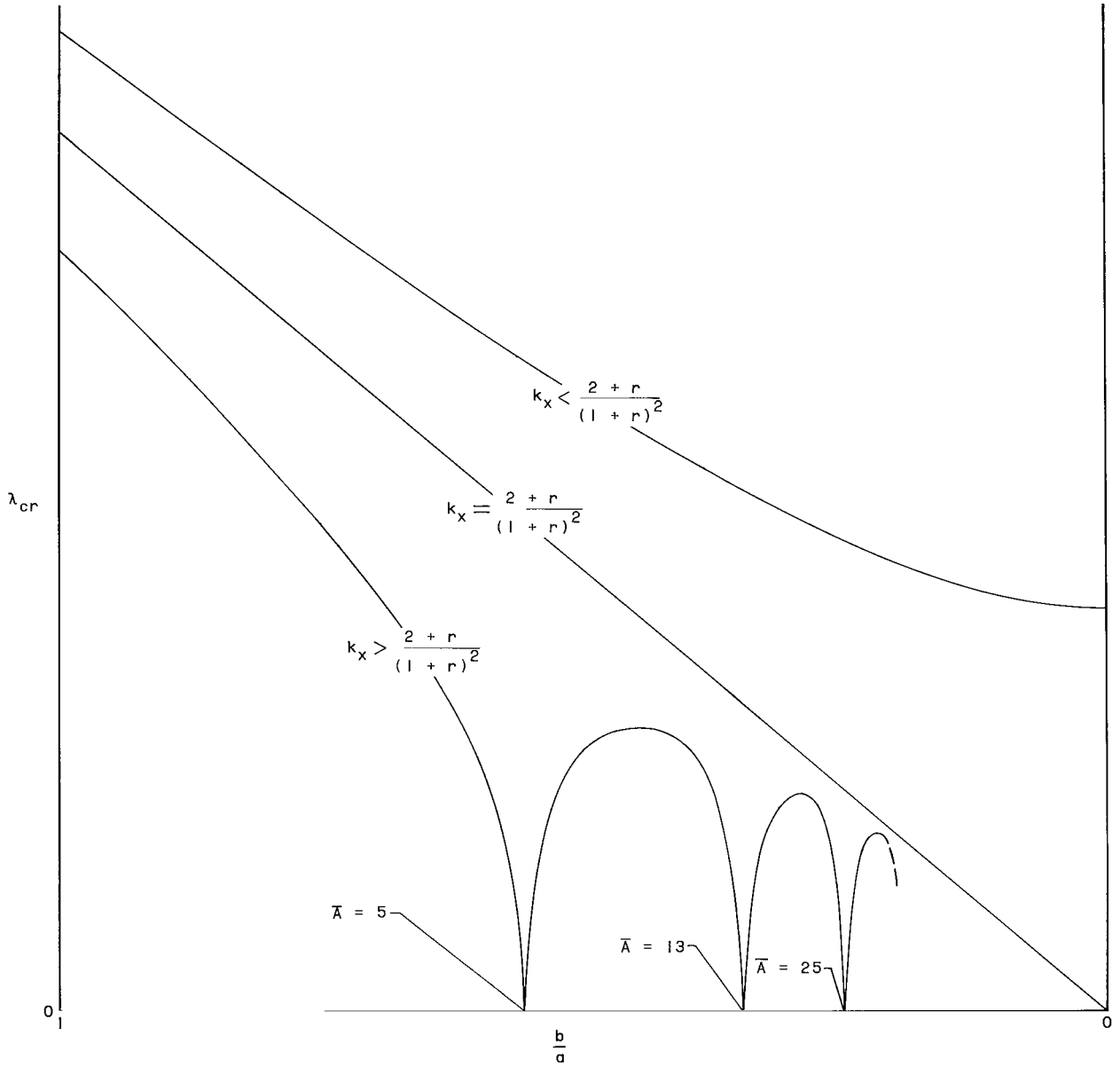

Figure 6.- Effect of stress on the flutter boundary for r constant.

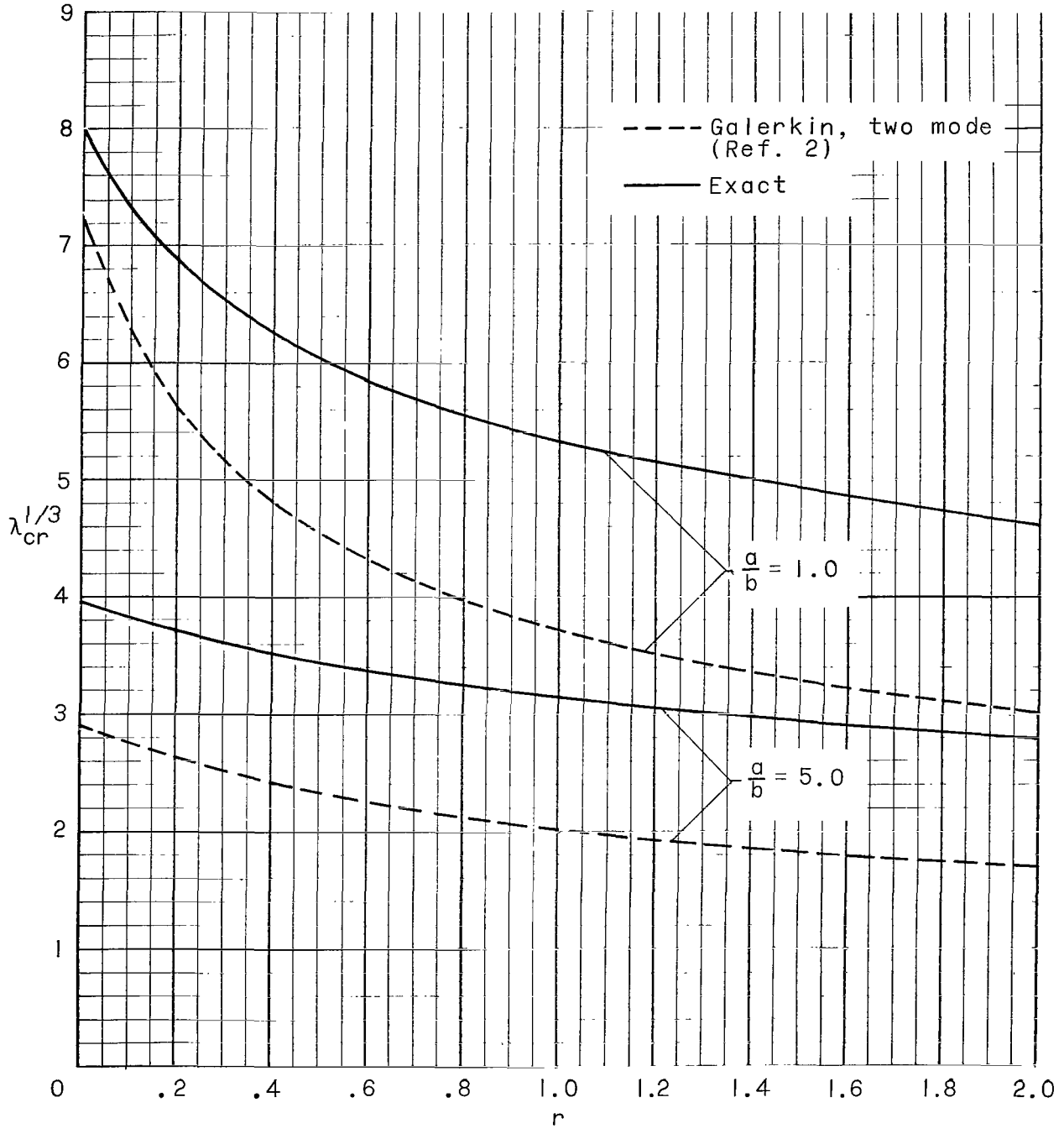

Figure 7.- Comparison of flutter boundaries from two-mode Galerkin solution and exact solution. $k_x = 0$.

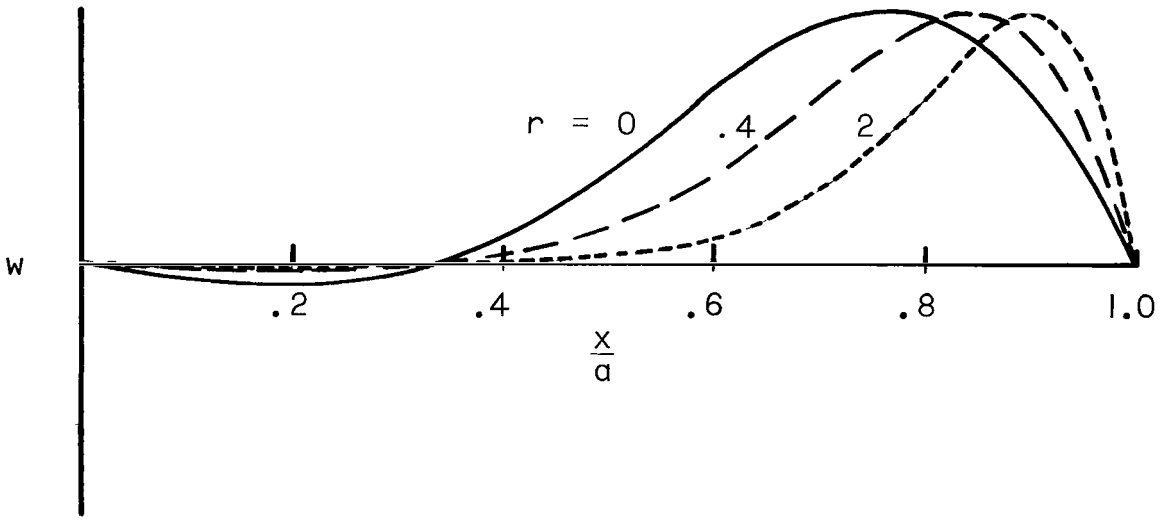

Figure 8.- Mode shape at flutter for an unstressed square sandwich panel. $a/b = 1$; $k_x = 0$.

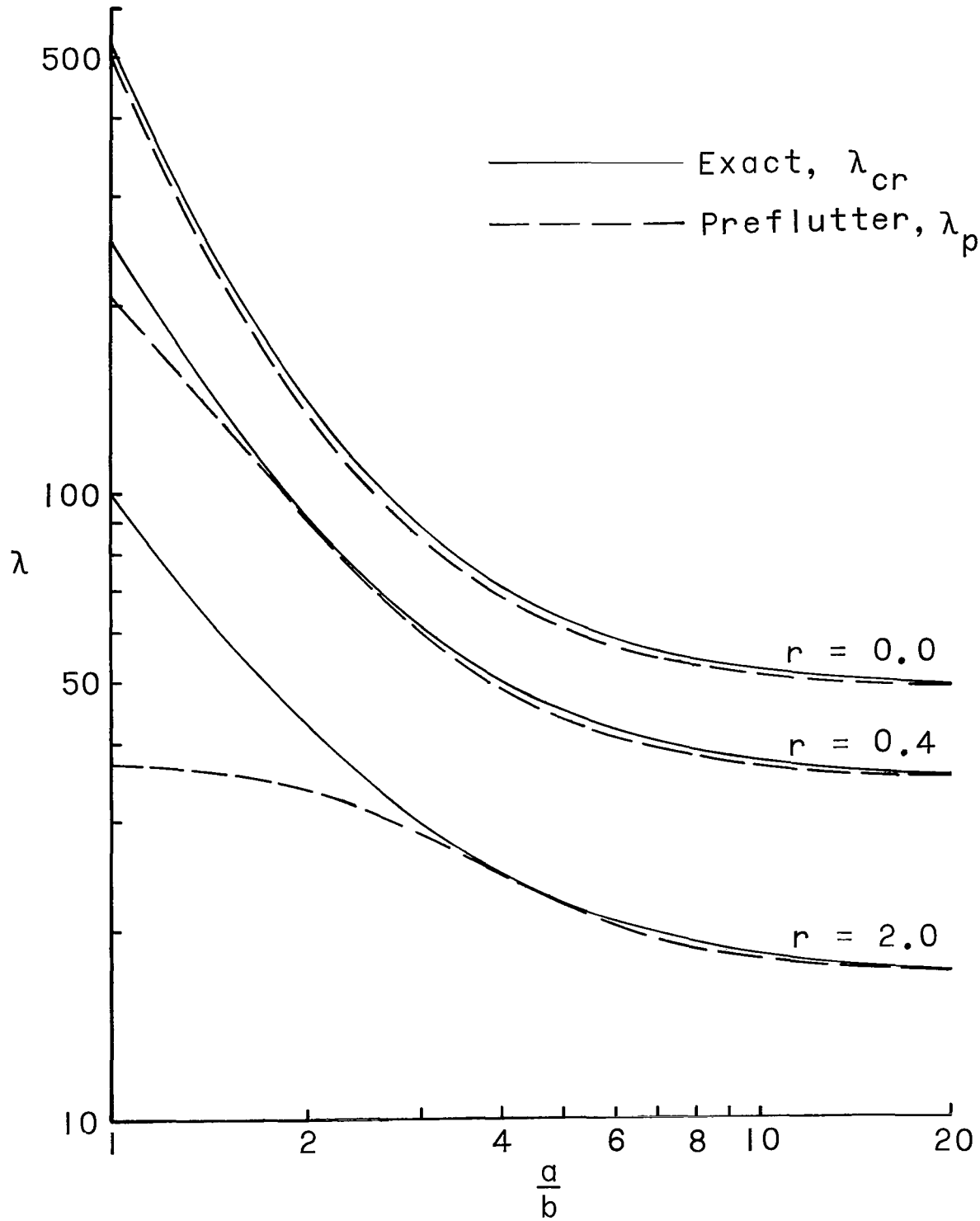

Figure 9.- Comparison of preflutter and exact flutter boundaries. $k_x = 0$.

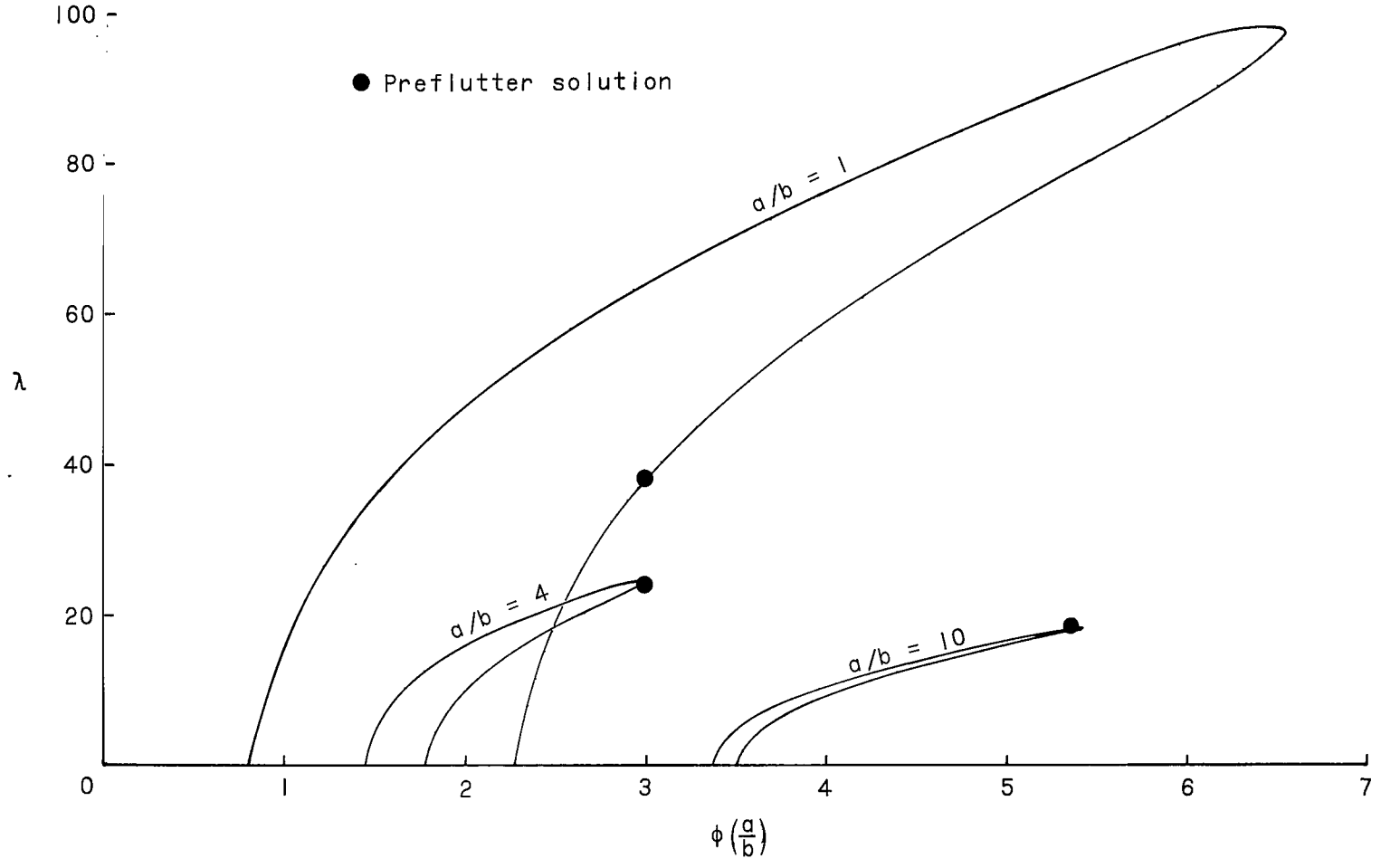

Figure 10.- Location of preflutter solution on frequency loops. $k_x = 0$; $r = 2$.

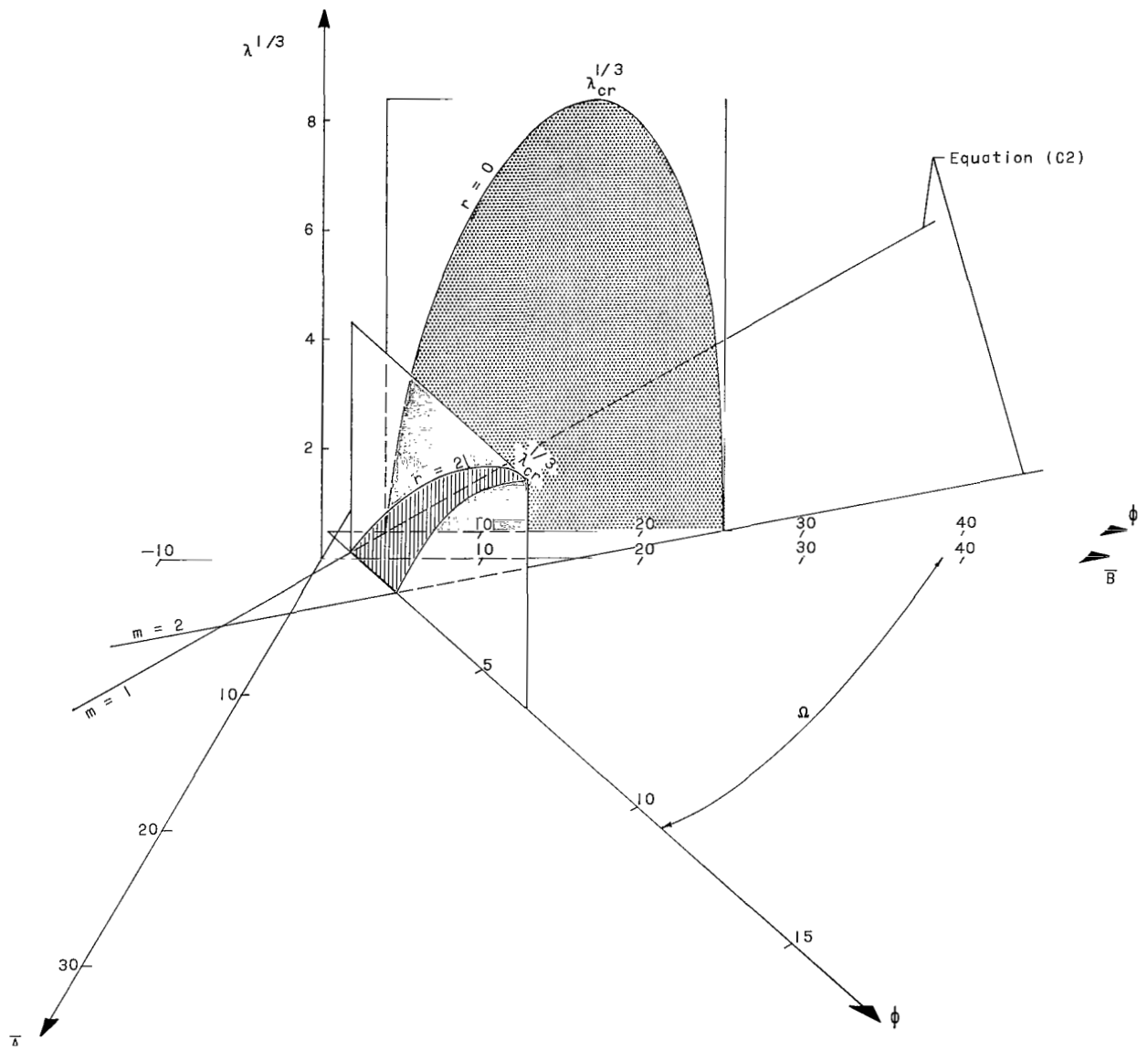

Figure 11.- Effect of transverse shear stiffness on the flutter solution. $a/b = 1$; $k_x = 0$.

3/2.2/PT

"The aeronautical and space activities of the United States shall be conducted so as to contribute . . . to the expansion of human knowledge of phenomena in the atmosphere and space. The Administration shall provide for the widest practicable and appropriate dissemination of information concerning its activities and the results thereof."

—NATIONAL AERONAUTICS AND SPACE ACT OF 1958

NASA SCIENTIFIC AND TECHNICAL PUBLICATIONS

TECHNICAL REPORTS: Scientific and technical information considered important, complete, and a lasting contribution to existing knowledge.

TECHNICAL NOTES: Information less broad in scope but nevertheless of importance as a contribution to existing knowledge.

TECHNICAL MEMORANDUMS: Information receiving limited distribution because of preliminary data, security classification, or other reasons.

CONTRACTOR REPORTS: Technical information generated in connection with a NASA contract or grant and released under NASA auspices.

TECHNICAL TRANSLATIONS: Information published in a foreign language considered to merit NASA distribution in English.

TECHNICAL REPRINTS: Information derived from NASA activities and initially published in the form of journal articles.

SPECIAL PUBLICATIONS: Information derived from or of value to NASA activities but not necessarily reporting the results of individual NASA-programmed scientific efforts. Publications include conference proceedings, monographs, data compilations, handbooks, sourcebooks, and special bibliographies.

Details on the availability of these publications may be obtained from:

SCIENTIFIC AND TECHNICAL INFORMATION DIVISION

NATIONAL AERONAUTICS AND SPACE ADMINISTRATION

Washington, D.C. 20546